



# 1 Investigating Carbonyl Compounds above the Amazon Rainforest 2 using PTR-ToF-MS with NO<sup>+</sup> Chemical Ionization

3 Akima Ringsdorf<sup>1</sup>, Achim Edtbauer<sup>1</sup>, Bruna Holanda<sup>2</sup>, Christopher Poehlker<sup>2</sup>, Marta O. Sá<sup>3</sup>,  
4 Alessandro Araújo<sup>4</sup>, Jürgen Kesselmeier<sup>2</sup>, Jos Lelieveld<sup>1,5</sup>, Jonathan Williams<sup>1,5</sup>

5 <sup>1</sup>Department of Atmospheric Chemistry, Max Planck Institute for Chemistry, Mainz, Germany

6 <sup>2</sup>Department of Multiphase Chemistry, Max Planck Institute for Chemistry, Mainz, Germany

7 <sup>3</sup>Instituto Nacional de Pesquisas da Amazonia (INPA), Manaus, CEP 69067-375, Brazil

8 <sup>4</sup>Empresa Brasileira de Pesquisa Agropecuária (Embrapa) Amazonia Oriental, Belem, CEP 66095-100, Brazil

9 <sup>5</sup>Climate and Atmosphere Research Center, The Cyprus Institute, 1645 Nicosia, Cyprus

10 *Correspondence to:* Jonathan Williams (J.Williams@mpic.de) and Akima Ringsdorf (A.Ringsdorf@mpic.de)

11 **Abstract.** The photochemistry of carbonyl compounds significantly influences tropospheric chemical composition by  
12 altering the local oxidative capacity, free radical abundance in the upper troposphere, and formation of ozone, PAN,  
13 and secondary organic aerosol particles. Carbonyl compounds can be emitted directly from the biosphere into the  
14 atmosphere and are formed through photochemical degradation of various precursor compounds. Aldehydes have  
15 atmospheric lifetimes of hours to days, in contrast to ketones, which persist for up to several weeks. While standard  
16 operating conditions for proton transfer time-of-flight mass spectrometer (PTR-ToF-MS) using H<sub>3</sub>O<sup>+</sup> ions are unable  
17 to separate aldehydes and ketones, the use of NO<sup>+</sup> reagent ions allows for the differential detection of isomeric  
18 carbonyl compounds with a high time resolution. Here we study the temporal (24 h) and vertical (80–325 m)  
19 variability of individual carbonyl compounds in the Amazon rainforest atmosphere with respect to their rainforest-  
20 specific sources and sinks. We found strong sources of ketones within or just above the rainforest canopy (acetone,  
21 MEK, and C<sub>5</sub>-ketones). A common feature of the carbonyls was nocturnal deposition observed by loss rates, most  
22 likely since oxidized volatile organic compounds are rapidly metabolized and utilized by the biosphere. With NO<sup>+</sup>  
23 chemical ionization, we show that the dominant carbonyl species include acetone and propanal, which are present at  
24 a ratio of 1:10 in the wet-to-dry transition and 1:20 in the dry season.

25

## 26 1 Introduction

27 On a global scale, tropical forests are regarded as the largest source of biogenic volatile organic compounds (BVOC)  
28 for the atmosphere (Guenther, 2013). BVOC comprise multiple compound classes including terpenes, alkenes,  
29 alkanes, alcohols, acids, esters, halocarbons, and carbonyls, all emitted as a result of various physiological processes,  
30 such as those occurring in plants, soils, etc., and as a function of environmental conditions. The emission quantity and  
31 composition vary among plant species, thus given the high biodiversity in tropical forests, the ecosystem composition  
32 and developmental stage also need to be considered as clearly demonstrated by Ciccioli et al. (2023). Most of the  
33 carbon released as BVOC from the tropical rainforest is in the form of terpenes, including the hemiterpene isoprene  
34 (C<sub>5</sub>H<sub>8</sub>) (Yáñez-Serrano et al., 2015), monoterpenes such as alpha-pinene (C<sub>10</sub>H<sub>16</sub>) (Zannoni et al., 2020b), and  
35 sesquiterpenes such as copaene (C<sub>15</sub>H<sub>24</sub>) (Yee et al., 2020). In addition, considerable amounts of oxygenated VOC  
36 (OVOC) are known to be present in rainforest air, with carbonyl compounds, namely aldehydes and ketones containing  
37 the C=O functional group, constituting an important subset of the atmospheric OVOC (Kesselmeier and Staudt, 1999).  
38 Direct biogenic emission, biomass burning, and secondary formation, mainly from the oxidation of the aforementioned  
39 terpene precursors and photolysis of larger carbonyls, all contribute to the cocktail of carbonyl compounds in the  
40 atmosphere (Guenther, 2013; Mellouki et al., 2015; Liu et al., 2022). To understand this cocktail, deposition and  
41 uptake by vegetation, i.e., bidirectional exchange, should always be considered as potential contributors (Kesselmeier,  
42 2001; Kesselmeier et al., 1997; Villanueva et al., 2014). The formation of carbonyl species occurs after the oxidation  
43 of VOC is initiated by the hydroxyl radical (OH), ozone (O<sub>3</sub>), or at nighttime by the nitrate radical (NO<sub>3</sub>), and the  
44 resulting peroxy radicals (RO<sub>2</sub>) react either with nitrogen oxide (NO) (when present) or with other ambient RO<sub>2</sub> or



45 HO<sub>2</sub> radicals. In the presence of NO this oxidation chain results in a net production of O<sub>3</sub>, an important radiatively  
46 active oxidant in the Amazon and worldwide (Mellouki et al., 2015; Trebs et al., 2012).

47 The main atmospheric carbonyl sinks are photolysis and oxidation by OH (Atkinson and Arey, 2003). As a  
48 consequence, reactions with carbonyls combined with those of other BVOC determine the availability of OH and thus  
49 the oxidative capacity of the atmosphere (Lelieveld et al., 2016). In Amazon rainforest air, OVOC account for 22-40 %  
50 of OH reactivity, namely the overall loss frequency of OH radicals (Pfanerstill et al., 2021). Unsaturated carbonyls,  
51 like the isoprene oxidation products methacrolein (MACR) and methyl vinyl ketone (MVK), are also oxidized by O<sub>3</sub>.  
52 Ketones, such as acetone, react much less readily with OH than aldehydes and, accordingly, have longer atmospheric  
53 lifetimes. Thus, they persist during long-range transport and convective lifting to high altitudes, whereas more reactive  
54 aldehydes impact the chemistry more locally. However, through rapid, deep convection, a frequent phenomenon in  
55 the humid and hot tropics, also aldehydes can be transported to altitudes between 10 and 17 km (Prather and Jacob,  
56 1997).

57 Oxidation of aldehydes and photolysis of ketones and dicarbonyls and further reaction with NO<sub>x</sub> (NO + NO<sub>2</sub>) yields  
58 peroxyacetic nitric anhydride (PAN). PAN and other peroxy nitrates are thermally unstable near the surface but  
59 in the cooler mid- and upper troposphere PAN is the most abundant reservoir for nitrogen oxides and is transported  
60 over long distances (Mellouki et al., 2015; Fischer et al., 2014; Singh et al., 1990; Roberts, 2007). The main precursors  
61 of PAN are acetaldehyde, followed by more minor contributions from methylglyoxal (not reported here) and acetone  
62 (Fischer et al., 2014). NO<sub>x</sub> in the tropical atmosphere originates from several processes, starting with microbial  
63 activities in soils and the release of NO, which is rapidly oxidized to NO<sub>2</sub>, a large fraction even before it escapes the  
64 canopy. NO<sub>2</sub> can be taken up by vegetation and only a part of this species traverses the canopy to the atmosphere  
65 above (Breuninger et al., 2013; Rummel et al., 2002; Chaparro-Suarez et al., 2011). Further sources are lightning  
66 discharges and biomass burning, the latter having the strongest seasonal variability (Bond et al., 2002).

67 The photochemical degradation of carbonyls in the atmosphere is also a source of HO<sub>x</sub> (HO<sub>2</sub> + OH) radicals,  
68 particularly important in the upper troposphere where OH radical production from carbonyls can exceed primary  
69 production in areas impacted by convection (Liu et al., 2022; Colomb et al., 2006; Lary and Shallcross, 2000; Prather  
70 and Jacob, 1997). Furthermore, the abundance of radicals and oxidation products of carbonyls and dicarbonyls can  
71 promote the formation and growth of secondary organic aerosols (Liu et al., 2022).

72 In this study, the observed diel and vertical (80-325 m) variability of 15 carbonyl species (C<sub>2</sub>-C<sub>9</sub>) was investigated.  
73 These species were detected online with a PTR-ToF-MS using NO<sup>+</sup> as a reagent ion. This technique enables the  
74 separation of isomeric aldehydes and ketones to identify their partitioning in the Amazonian atmospheric boundary  
75 layer (ABL) at the ATTO site. Previous measurements of carbonyls have been conducted over the rainforest using  
76 PTR-MS with H<sub>3</sub>O<sup>+</sup> as the reagent ion (Yáñez-Serrano et al., 2016). With this method, both aldehyde and ketone  
77 carbonyl forms are detected at the same mass. Usually, for airborne measurements, atmospheric chemists have argued  
78 that the m/z used for the detection of C<sub>3</sub> carbonyls can be interpreted to be predominantly acetone since its atmospheric  
79 lifetime is relatively long (Williams et al., 2001). However, near biogenic sources, the fractional distribution can be  
80 different, and especially if the data is used to extract further information about the environment, such as OH  
81 concentrations (Williams et al., 2000), the validity of this assumption should be verified.

82 The dataset presented here is the first online measurement of speciated individual aldehydes and ketones in the  
83 Amazon. This rainforest environment is characterized by high solar insolation and vigorous vertical transport by deep  
84 convection. In quantifying the relative abundance of carbonyl species, we aimed to improve the understanding of their  
85 emissions, secondary formation in the atmosphere, transformation, and deposition in the Amazon rainforest region.

## 86 **2 Experimental**

### 87 **2.1 Measurement site and instrumentation**

88 All measurements were conducted at the Amazon Tall Tower Observatory (ATTO) within the primary tropical  
89 rainforest of Brazil. The site is located 135 km NE of Manaus (02.14°S, 58.99°W, 120 m above sea level) with the  
90 main wind direction being NE to SE (Fig. S1). In the wet season (February–May), the air is typically nearly pristine



91 since the air masses pass over more than 1000 km of mostly unperturbed rainforest before being sampled, with a  
92 possible influence due to long-range transport from African biomass burning pollution, which has been observed in  
93 the beginning of the dry season (February–March) (Holanda et al., 2023). This is reflected by low concentrations of  
94 NO<sub>x</sub> of less than 150 ppt in the ABL during the late wet season. In the dry season (August–November), however, air  
95 influenced by mainly man-made biomass burning in South America was observed. In the same season enhanced black  
96 carbon concentrations were measured due to the hemispheric wide summer maximum in biomass burning. The site  
97 hosts a 325-m-tall tower and an 80-m walk-up tower, among other measurement and accommodation facilities. A  
98 detailed map can be found in the Supplement (Fig. S2). The canopy height of the surrounding forest is about 35 m  
99 (Kuhn et al., 2007). A comprehensive description of the site is provided by Andreae et al. (2015). The measurements  
100 described here were conducted from June 23 until July 8 and from September 27 until October 14, 2019.

101 The sampling inlets for the BVOC measurements are located at 80, 150, and 325 m on the tall tower. Air is drawn by  
102 high-volume pumps down to the instrumentation that is stored in an air-conditioned container at the foot of the tower.  
103 By sequentially sampling each height for 5 minutes, a semi-continuous measurement can be achieved, so that each  
104 height is sampled four times per hour. The flow in the insulated and heated (40 °C) Teflon sampling lines (3/8"OD)  
105 is about 10 l min<sup>-1</sup>. A long inlet line can be compared to a gas chromatographic column, which retains the sampled  
106 VOC depending on their volatility and polarity, expressed by a wall saturation concentration (Pagonis et al., 2017).  
107 Adsorption to the inner walls of the Teflon line caused a response time of 90 seconds at ATTO using a VOC gas  
108 standard. Before the actual sampling of each height, the line was therefore flushed with ambient air to achieve  
109 saturation. Tests with a 400-m inlet line in China have shown that the carbonyl compounds investigated in this study  
110 have high saturation concentrations (C\*, which is inversely proportional to the wall partitioning) and are not affected  
111 by line loss (Li et al., 2023; Deming et al., 2019), but line effects such as a broadening of initially sharp concentration  
112 peaks cannot be excluded. It has to be noted that sharp concentration peaks or spikes of short duration (< 90 s) were  
113 not expected high above the homogenous vegetation of the rainforest. Some less volatile molecules, like  
114 sesquiterpenes, never reached saturation and were additionally potentially degraded by O<sub>3</sub> or NO<sub>3</sub> (which was shown  
115 to form inside the insulated tubing (Li et al., 2023)); thus, they were not detected. A potential contribution from the  
116 oxidation of sesquiterpenes inside the tubing to detected carbonyl species cannot be excluded; however, this  
117 contribution is expected to be minor given the rapidly decreasing sesquiterpene concentrations with increasing  
118 distance from the canopy (Yee et al., 2018). The residence time in the tubing is short compared to the time that  
119 sesquiterpenes are exposed to oxidation during atmospheric transport before reaching the sampling heights. VOC were  
120 measured by a Proton Transfer Reaction Time of Flight Mass Spectrometer (PTR-ToF-MS 4000, Ionicon Analytik,  
121 Innsbruck, Austria) (Jordan et al., 2009) with a time resolution of 20 seconds.

122 Meteorological data were measured at the walk-up tower at multiple heights up to 80 m (LI7500A, LI-COR  
123 Biotechnology, Lincoln, USA) and at the tall tower at 325 m (Lufft, WS600-LMB, G. Lufft Mess- und Regeltechnik  
124 GmbH, Fellbach, Germany) with a time resolution of 1 minute.

125

## 126 2.2 NO<sup>+</sup> chemical ionization

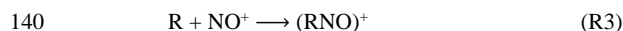
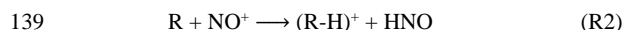
127 PTR-ToF-MS in general is a form of chemical ion mass spectrometry (CIMS) commonly operated with hydronium  
128 ions (H<sub>3</sub>O<sup>+</sup>) for the chemical ionization of VOC in air samples. The technique is well-established and sensitive and is  
129 able to detect most of the prominent VOC in ambient air with a high temporal resolution of seconds (de Gouw and  
130 Warneke, 2007). The proton transfer reaction that lends its name to the instrument occurs between H<sub>3</sub>O<sup>+</sup> ions and the  
131 molecules R with a higher proton affinity than water (> 691 kJ mol<sup>-1</sup>) (Hunter and Lias, 1998).



133 Thus, isomeric molecules (such as acetone and propanal) form the same product ion RH<sup>+</sup> and cannot be distinguished.  
134 For the purpose of investigating the atmospheric chemistry of carbonyl compounds, this is a major disadvantage since  
135 the distribution between short-lived aldehydes and longer-lived ketones with the same carbon number remains unclear.  
136 However, it has been shown that by using an alternative reagent ion (i.e., NO<sup>+</sup>), aldehydes and ketones can be



137 distinguished.  $\text{NO}^+$  ionizes aldehydes mainly via hydride abstraction (R2), whereas ketones and  $\text{NO}^+$  tend to form a  
138 cluster (R3) leading to different product ions (Koss et al., 2016; Španěl et al., 1997).



141 To implement the  $\text{NO}^+$  chemical ionization mass spectrometer ( $\text{NO}^+$  CIMS), synthetic air instead of water vapor was  
142 introduced in the ion source, and the source parameters were tuned to achieve a low contribution of impurity ions  
143 ( $\text{H}_3\text{O}^+$ ,  $\text{O}_2^+$ ,  $\text{NO}_2^+$ ) and high counts of  $\text{NO}^+$ . The identity of the reaction that occurs to ionize the target compound  
144 depends on the thermodynamical properties of the molecule. The hydride ion affinity of aldehydes is less than that of  
145  $\text{NO}^+$ , so R2 is exothermic and favored (Karl et al., 2012; Španěl et al., 1997). Ketones do not show the same tendency  
146 to donate a hydrogen atom and the ionization energies of most ketones, especially small ones, is slightly higher than  
147 that of  $\text{NO}$  ( $> 9.26$  eV) (Smith et al., 2003). Thus, an association reaction, R3, primarily occurs for the ketones in this  
148 study. Due to the humid conditions in the rainforest,  $\text{NO}^+(\text{H}_2\text{O})$ -clusters were also available to react with ketones via  
149 ligand switching, producing the same products as the association reaction R3 (Smith et al., 2003). The ionization  
150 energies of 3-hexanone, 2-heptanone, and 2-nonanone are smaller than or equal to that of  $\text{NO}$ ; nevertheless, the  
151 association reaction has been shown to be favored by selected ion flow tube (SIFT) studies (Španěl et al., 1997). Those  
152 compounds were, however, not detected in the mass spectra obtained in the rainforest environment examined in this  
153 study.

154 Besides the most favored reaction, other ionization channels can also produce product ions. This, and partial  
155 fragmentation in the drift tube can lead to additional complications of the mass spectra. To identify the distribution of  
156 product ions and fragments of carbonyls for the type of instrument used in this study, a single-compound headspace  
157 analysis was performed in the laboratory using a PTR-ToF-MS 8000. The basic components of the instrument, mainly  
158 the ion source, drift tube, and detector are similar to a PTR-ToF-MS 4000, so that the relative transmission can be  
159 assumed to be identical. The instrument was tuned to have the same E/N (electric field intensity divided by gas number  
160 density) in the drift tube and similar impurities ( $\leq 5\%$ ) as the instrument in the field. In both field and laboratory, two  
161 different settings for the E/N values were applied. One set had a relatively low E/N of 70 Td, which has been  
162 recommended in previous studies to minimize fragmentation (Koss et al., 2016; Romano and Hanna, 2018); the other  
163 was operated with 120 Td for comparison. The results of the single-compound headspace analysis can be found in the  
164 Supplementary (Table S1).

165 The complexity of the mass spectra measured with a  $\text{NO}^+$  CIMS is a disadvantage if one aims for a non-targeted  
166 analysis of VOC present in a certain environment, such as the rainforest. Long-term VOC observations at ATTO are  
167 therefore conducted with a PTR-ToF-MS using  $\text{H}_3\text{O}^+$  ions. However, for a targeted analysis, specifically for separating  
168 carbonyl compounds, the  $\text{NO}^+$  CIMS is a convenient method (Koss et al., 2016; Karl et al., 2012; Ernle et al., 2023).  
169 Another advantage of the  $\text{NO}^+$  chemistry is the ability to detect certain alkanes, as their proton affinity is too low to  
170 be detected by a PTR-MS (Koss et al., 2016). This has been widely used in urban or rural areas to quantify vehicle  
171 emissions, but such species have not yet been investigated at the ATTO rainforest site (Wang et al., 2020a; Chen et  
172 al., 2022).

173

### 174 **2.3 VOC data analysis**

175 Integration of the mass spectra, baseline-, and duty-cycle-correction were performed using the IDA software (Ionicon  
176 Analytik). In a subsequent step, the obtained signals were normalized to  $\text{NO}^+$  and  $\text{H}_2\text{ONO}^+$  and drift parameters like  
177 pressure and temperature, to account for fluctuations.

178 Table 1 shows the sensitivities and limits of detection (LoD) for all target molecules with E/N values of 70 and 120 Td  
179 applied. It was evident that the sensitivity of ketones decreases dramatically with high E/N conditions, most probably  
180 due to enhanced fragmentation caused by more collisions in the drift tube.



181 Compounds displayed in bold in Table 1 were quantified using a primary VOC gas standard (Apel-Riemer  
182 Environmental Inc., Colorado, USA). Unfortunately, this did not comprise all target carbonyls, and for those  
183 compounds not in the standard, a theoretical method was applied to obtain concentrations, resulting in a higher  
184 uncertainty. The relative distribution of the product ions obtained from the single-compound headspace analysis was  
185 used to correct for the fragmentation of carbonyl compounds with higher  $m/z$ -ratios onto the parent  $m/z$ -ratios of other  
186 target compounds.

187 For those compounds not included in the gas standard, mixing ratios were obtained by calculating the ionization  
188 efficiency with a previously determined reaction rate of  $\text{NO}^+$  and the target compound under the current conditions in  
189 the drift tube (k-rate analysis) (Cappellin et al., 2012). The reaction rates (k-rates), also presented in Table 1, have  
190 been derived for the sum of all product ions. Thus, a weighting factor for the relative production of the target ion  
191 needed to be applied, which was also obtained by the single-compound headspace analysis from the slope of the  
192 signals of the target ion vs. other product ions. The mixing ratios of both E/N settings, obtained by applying the  
193 respective product ion distributions, agree well for most compounds (except for n-hexanal and ketones, which have a  
194 low sensitivity at 120 Td). This accordance supports the assumption that product ion distributions were valid for both  
195 instruments. To calculate propanal, the calibration factor of methacrolein was used, since in a previous calibration  
196 measurement with the PTR-ToF-MS 8000 both compounds had similar sensitivities (methacrolein:  $0.13 \text{ ppb ncps}^{-1}$ ,  
197 propanal:  $0.17 \text{ ppb ncps}^{-1}$ ).

198 The measurement uncertainty in the mixing ratios of standard calibrated VOC was less than 25%. It was derived from  
199 the accuracy of the VOC gas standard ( $\pm 5\%$ ), the flow meter used for the calibration ( $\pm 1\%$ ), the accuracy of the least  
200 square fit of the calibration curve (molecule-dependent, circa  $\pm 10\%$ ), and the uncertainty of the relative distribution  
201 of product ions, which was expected to be below 20%. The uncertainty of the product ion distribution was estimated  
202 from the purity of the liquid carbonyls tested ( $> 95\%$ ) as well as possible contamination during the headspace  
203 sampling. In the case of theoretically calculated mixing ratios using k-rates the accuracy was accordingly higher. The  
204 accuracy of the k-rate ( $\pm 20\%$ ) (Španěl et al., 1997) and the accuracy of the distribution of product ions give the  
205 absolute accuracy for k-rate calibrated mixing ratios which was thus estimated to be below 30%.

206 Detection limits were defined as three times the standard deviation of the background noise at the specified mass.  
207 Those are also displayed in Figures 1–2. Negative values arising from the subtraction of the background were set to  
208 zero to account for a slightly too high background measurement of some compounds during calibration.

209

#### 210 **2.4 Validation of observations**

211 Pre-separation of the VOC with a GC column prior to detection with the  $\text{NO}^+$  CIMS can indicate the pureness or  
212 compound specificity of an  $m/z$  ratio. Koss et al., 2016 reported such data for urban ambient air and concluded that  
213 certain masses can be seen as unambiguous in that environment. The E/N field used in that study, which strongly  
214 impacts the fragmentation patterns on different  $m/z$  ratios, was similar to this study (60 Td), but the measurement site  
215 was a parking lot in an urban area (Koss et al., 2016). Uncontaminated  $m/z$  ratios assigned to carbonyl compounds  
216 were found for acetaldehyde, propanal, methacrolein, and crotonaldehyde, the sum of  $\text{C}_5$ -aldehydes, acetone, hexanal,  
217 MVK, methyl ethyl ketone (MEK), benzaldehyde, heptanal, the sum of  $\text{C}_5$ -ketones, and octanal. Nevertheless,  
218 biogenic compounds that may not be present in an urban environment were, therefore, not part of the GC method  
219 applied in Koss et al. and remained as potential interferents for the carbonyl  $m/z$  ratios.

220 Allyl ethyl ether, an isomer of  $\text{C}_5$ -carbonyls that also undergoes hydride transfer, was potentially such a candidate for  
221 interfering in the  $\text{C}_5$ -aldehyde  $m/z$  ratio. (Smith et al., 2011; Španěl and Smith, 1998). The  $m/z$  ratio of  $\text{C}_5$ -aldehydes  
222 might have also been affected by 1-5 pentanediol if present at significant concentrations (Španěl et al., 2002). Some  
223 carboxylic acids react with  $\text{NO}^+$  under the drift tube conditions to form  $\text{R} - \text{OH} + \text{HNO}_2$  and thus make isomers to the  
224 ionized carbonyl species. Trimethylacetic acid was reported to mainly form  $\text{C}_5\text{H}_9\text{O}^+$  and thus can also potentially  
225 interfere with  $\text{C}_5$ -aldehydes (Španěl and Smith, 1998).

226 N-butyric acid is part of the glucose metabolism in plants and, upon ionization, partly makes  $\text{C}_4\text{H}_7\text{O}^+$  ions ( $m/z$   
227 71.0491); thus, it potentially interfered with butanal (Smith et al., 2011). The same holds for isobutyric acid. Also,



228 valeric acid has been shown to fragment into  $C_4H_7O^+$  to a great extent (Španěl and Smith, 1998). For the alcohols 2-  
229 butanol, 1,4-butanediol, and the ester methyl butyrate, fragmentation into  $C_4H_7O^+$  has been shown to occur (Koss et  
230 al., 2016; Španěl et al., 2002; Španěl and Smith, 1998). Tetrahydrofuran, an ether isomeric with butanal is ionized via  
231 hydride transfer and also forms  $C_4H_7O^+$  (Španěl and Smith, 1998). Contamination from 2-butanol was shown to  
232 account for around 50% of  $C_4H_7O^+$  at an urban site in Boulder, USA (Koss et al., 2016). Since 2-butanol has been  
233 previously found in emissions from vegetation (Kesselmeier and Staudt, 1999) and the mixing ratios of  $C_4H_7O^+$  were  
234 close to the detection limit, butanal could not be investigated without potential bias from other oxygenated VOC. With  
235 another measurement technique (sampling to adsorbent tubes and measurement with a GC-ToF-MS) applied at ATTO  
236 also no significant butanal peak was found. However, butanal has been identified in the Amazonian atmosphere during  
237 the dry and wet seasons at another site in 1999 (Andreae et al., 2002).



**Table 1: List of identified carbonyl compounds and other hydrocarbons and their properties for detection with NO<sup>+</sup> CIMS (PTR-ToF-MS 4000). Sensitivities are compared to the classical PTR-MS method using H<sub>3</sub>O<sup>+</sup> reagent ions. The “product factor” represents the weighting factor for the k-rate obtained from the distribution of product ions as described in section 2.3. Compounds in bold were quantified using a primary standard.**

| Carbonyl species              | Ion formula   | Exact m/z | k-rate<br>10 <sup>-9</sup> cm <sup>3</sup> s <sup>-1</sup> | NO <sup>+</sup> |                                       |            |              |                                       |            | H <sub>3</sub> O <sup>+</sup> |                                       |
|-------------------------------|---|-----------|--|-----------------|---------------------------------------|------------|--------------|---------------------------------------|------------|-------------------------------|---------------------------------------|
|                               |   |           |  | Prod. factor    | E/N = 70 Td                           |            |              | E/N = 120 Td                          |            |                               | Sensitivity<br>ppb ncps <sup>-1</sup> |
|                               |   |           |  |                 | Sensitivity<br>ppb ncps <sup>-1</sup> | LoD<br>ppb | Prod. factor | Sensitivity<br>ppb ncps <sup>-1</sup> | LoD<br>ppb |                               |                                       |
| <b>Acetaldehyde</b>           | C <sub>2</sub> H <sub>3</sub> O <sup>+</sup>                | 43.01784  | 0.6(Španěl et al., 1997)                                   | -               | 0.155                                 | 0.112      | -            | 0.431                                 | 0.160      | 0.025                         |                                       |
| <b>Acetone</b>                | C <sub>3</sub> H <sub>6</sub> NO <sub>2</sub> <sup>+</sup>  | 88.0393   | 1.2(Španěl et al., 1997)                                   | (0.43)          | 0.078                                 | 0.06       | 0.27         | 4.803                                 | 0.705      | 0.031                         |                                       |
| <b>Propanal</b>               | C <sub>3</sub> H <sub>5</sub> O <sup>+</sup>                | 57.0335   | 2.5(Španěl et al., 1997)                                   | (0.79)          | <i>0.046</i>                          | 0.053      | 0.82         | <i>0.256</i>                          | 0.049      | -                             |                                       |
| <b>MEK</b>                    | C <sub>4</sub> H <sub>8</sub> NO <sub>2</sub> <sup>+</sup>  | 102.055   | 2.8(Španěl et al., 1997)                                   | (0.84)          | 0.049                                 | 0.008      | 0.61         | 1.027                                 | 0.111      | 0.028                         |                                       |
| MVK                           | C <sub>4</sub> H <sub>6</sub> NO <sub>2</sub> <sup>+</sup>  | 100.039   | 2.4(Michel et al., 2005)                                   | 0.86            | -                                     | 0.004      | 0.67         | -                                     | 0.012      | -                             |                                       |
| <b>MACR</b>                   | C <sub>4</sub> H <sub>5</sub> O <sup>+</sup>                | 69.03349  | 2.6(Michel et al., 2005)                                   | (0.54)          | 0.046                                 | 0.021      | 0.42         | 0.256                                 | 0.093      | 0.028                         |                                       |
| n-pentanone                   | C <sub>5</sub> H <sub>10</sub> NO <sub>2</sub> <sup>+</sup> | 116.0706  | 3.4(Španěl et al., 1997)                                   | 0.85            | -                                     | 0.005      | 0.56         | -                                     | 0.007      | -                             |                                       |
| n-pentanal                    | C <sub>5</sub> H <sub>9</sub> O <sup>+</sup>                | 85.0648   | 3.2(Španěl et al., 1997)                                   | 0.79            | -                                     | 0.003      | 0.28         | -                                     | 0.011      | -                             |                                       |
| n-hexanone                    | C <sub>6</sub> H <sub>12</sub> NO <sub>2</sub> <sup>+</sup> | 130.0863  | 3.3(Španěl et al., 1997)                                   | -               | -                                     | 0.002      | -            | -                                     | -          | -                             |                                       |
| Hexanal                       | C <sub>6</sub> H <sub>11</sub> O <sup>+</sup>               | 99.0804   | 2.5(Španěl et al., 1997)                                   | 0.75            | -                                     | 0.006      | 0.4          | -                                     | 0.016      | -                             |                                       |
| Trans-2-hexenal               | C <sub>6</sub> H <sub>9</sub> O <sup>+</sup>                | 97.0672   | 2.8(Roberts et al., 2022)                                  | 0.68            | -                                     | 0.006      | 0.82         | -                                     | 0.005      | -                             |                                       |
| Benzaldehyde                  | C <sub>7</sub> H <sub>5</sub> O <sup>+</sup>                | 105.033   | 2.8(Španěl et al., 1997)                                   | 0.96            | -                                     | 0.005      | 0.97         | -                                     | 0.003      | -                             |                                       |
| Heptanal                      | C <sub>7</sub> H <sub>13</sub> O <sup>+</sup>               | 113.0961  | 2  | -               | -                                     | 0.004      | -            | -                                     | 0.007      | -                             |                                       |
| Octanal                       | C <sub>8</sub> H <sub>15</sub> O <sup>+</sup>               | 127.1117  | 2.7(Romano and Hanna, 2018)                                | 0.81            | -                                     | 0.004      | 0.61         | -                                     | 0.004      | -                             |                                       |
| Nonanal                       | C <sub>9</sub> H <sub>17</sub> O <sup>+</sup>               | 141.1274  | 1.1(Roberts et al., 2022)                                  | 0.04            | -                                     | 0.145      | 0.1          | -                                     | 0.078      | -                             |                                       |
| Nopinone                      | C <sub>9</sub> H <sub>14</sub> O <sup>+</sup>               | 138.1039  | 2  | -               | -                                     | 0.019      | -            | -                                     | 0.002      | -                             |                                       |
| <i>Alkanes</i>                |   |           |  |                 |                                       |            |              |                                       |            |                               |                                       |
| Isopentane                    | C <sub>5</sub> H <sub>11</sub> <sup>+</sup>                 | 71.086    | 2  | -               | -                                     | 0.013      | -            | -                                     | 0.027      | -                             |                                       |
| Methylcyclopentane            | C <sub>6</sub> H <sub>11</sub> <sup>+</sup>                 | 83.086    | 2  | -               | -                                     | 0.005      | -            | -                                     | 0.008      | -                             |                                       |
| 2-, 3-methylpentane           | C <sub>6</sub> H <sub>13</sub> <sup>+</sup>                 | 85.101    | 2  | -               | -                                     | 0.007      | -            | -                                     | 0.006      | -                             |                                       |
| C <sub>7</sub> cyclic alkanes | C <sub>7</sub> H <sub>13</sub> <sup>+</sup>                 | 97.101    | 2  | -               | -                                     | 0.004      | -            | -                                     | 0.003      | -                             |                                       |





**Table 1 continued.**

| VOC species                                  | Ion formula  | Exact m/z | k-rate $10^{-9} \text{ cm}^3 \text{ s}^{-1}$ | NO <sup>+</sup> |                                    |         |              |                                    |         | H <sub>3</sub> O <sup>+</sup>      |
|--|--|-----------|--|-----------------|------------------------------------|---------|--------------|------------------------------------|---------|------------------------------------|
|  |  |           |  | E/N = 70 Td     |                                    |         | E/N = 120 Td |                                    |         | E/N = 120 Td                       |
|  |  |           |  | Prod. factor    | Sensitivity ppb ncps <sup>-1</sup> | LoD ppb | Prod. factor | Sensitivity ppb ncps <sup>-1</sup> | LoD ppb | Sensitivity ppb ncps <sup>-1</sup> |
| C2-alkyl-cyclohexanes                        | C <sub>8</sub> H <sub>15</sub> <sup>+</sup>                | 111.117   | 2  | -               | -                                  | 0.004   | -            | -                                  | 0.005   | -                                  |
| <i>Alkenes</i>                               |  |           |  |                 |                                    |         |              |                                    |         |                                    |
| C <sub>5</sub> -alkene (2-pentenes)          | C <sub>5</sub> H <sub>10</sub> <sup>+</sup>                | 70.0777   | 2  | -               | -                                  | -       | -            | -                                  | 0.009   | -                                  |
| C <sub>5</sub> -alkene (α-olefin)            | C <sub>5</sub> H <sub>10</sub> NO <sup>+</sup>             | 100.076   | 2  | -               | -                                  | 0.006   | -            | -                                  | 0.003   | -                                  |
| C <sub>6</sub> H <sub>10</sub>               | C <sub>6</sub> H <sub>10</sub> <sup>+</sup>                | 82.0777   | 2  | -               | -                                  | 0.006   | -            | -                                  | 0.01    |                                    |
| <i>Alcohols</i>                              |  |           |  |                 |                                    |         |              |                                    |         |                                    |
| Ethanol                                      | C <sub>2</sub> H <sub>5</sub> O <sup>+</sup>               | 45.0335   | 2  | -               | -                                  | 0.050   | -            | -                                  | 0.019   | -                                  |
| <i>Alkyne</i>                                |  |           |  |                 |                                    |         |              |                                    |         |                                    |
| Propyne                                      | C <sub>4</sub> H <sub>6</sub> <sup>+</sup>                 | 54.046    | 2  | -               | -                                  | 0.026   | -            | -                                  | 0.011   | -                                  |
| <i>Aromatic</i>                              |  |           |  |                 |                                    |         |              |                                    |         |                                    |
| <b>Benzene</b>                               | C <sub>6</sub> H <sub>6</sub> <sup>+</sup>                 | 78.046    | -  | -               | 0.101                              | 0.020   | -            | 0.071                              | 0.009   | 0.063                              |
| <i>Terpenes</i>                              |  |           |  |                 |                                    |         |              |                                    |         |                                    |
| <b>Isoprene</b>                              | C <sub>5</sub> H <sub>8</sub> <sup>+</sup>                 | 68.0621   | -  | -               | 0.078                              | 0.018   | -            | 0.068                              | 0.023   | 0.045                              |
| <b>Sum of mono-terpenes</b>                  | C <sub>10</sub> H <sub>16</sub> <sup>+</sup>               | 136.125   | -  | -               | 0.067                              | 0.004   | -            | 0.554                              | 0.039   | 0.103                              |
| <i>Other</i>                                 |  |           |  |                 |                                    |         |              |                                    |         |                                    |
| Furan  | C <sub>4</sub> H <sub>4</sub> O <sup>+</sup>               | 68.0258   | 2  | -               | -                                  | 0.008   | -            | -                                  | -       | -                                  |
| C <sub>5</sub> H <sub>4</sub> O <sub>3</sub> | C <sub>5</sub> H <sub>4</sub> NO <sub>4</sub> <sup>+</sup> | 142.014   | 2  | -               | -                                  | 0.005   | -            | -                                  | 0.003   | -                                  |

239 Propionic acid is a potential contaminant for propanal on the m/z of C<sub>3</sub>H<sub>5</sub>O<sup>+</sup>, but only a fraction of the acid was found  
 240 to land on the propanal m/z (Španěl and Smith, 1998). A higher fraction of the fragments of methyl and ethyl  
 241 propionate were detected as isomers to ionized propanal but have not been found to be present in biogenic emissions  
 242 so far (Španěl and Smith, 1998; Kesselmeier and Staudt, 1999).

243 It can also not be excluded that fragmentation to C<sub>2</sub>H<sub>3</sub>O<sup>+</sup> of several species, in particular acetic acid, methyl formate,  
 244 methyl acetate, and ethyl acetate contributes to the m/z ratio of acetaldehyde (C<sub>2</sub>H<sub>3</sub>O<sup>+</sup>). Experimental evidence for the  
 245 contamination has only been found for a small contribution of methyl and ethyl acetate of less than 20% (Španěl and  
 246 Smith, 1998).

247 The isomers hexanal and z-3-hexenol are known to be emitted together by damaged green leaves (Langford et al.,  
 248 2010; Jardine et al., 2012a). A possible detection of both compounds on m/z of C<sub>6</sub>H<sub>11</sub>O<sup>+</sup> could not be excluded, since  
 249 alcohols also undergo hydride abstraction during the reaction with NO<sup>+</sup> (Koss et al., 2016).

250 To our knowledge, none of the species that were demonstrated to fragment on the same m/z ratios as carbonyls have  
 251 been reported to be abundant in forested environments or even to be biogenically emitted, except for z-3-hexenol, 2-  
 252 butanol, n- and isobutyric acid, acetic acid, and propionic acid. In general, acids have primary sources, including  
 253 biogenic emissions and biomass burning but also photochemical sources including the ozonolysis of alkenes  
 254 (Orzechowska et al., 2005). The dataset from this study and comparison with the corresponding m/z of acids under





255 H<sub>3</sub>O<sup>+</sup> ionization that have been measured previously at the ATTO site suggested that carboxylic acids undergo an  
256 association reaction with NO<sup>+</sup>. A headspace analysis with acetic acid also revealed no significant contributions to any  
257 other m/z except the association product C<sub>2</sub>H<sub>4</sub>NO<sub>3</sub><sup>+</sup>.

258 Fragmentation from higher carbonyls to m/z ratios attributed to lower carbonyls was observed in the single compound  
259 headspace analysis, conducted with aldehydes and ketones up to nonanal. The m/z of acetaldehyde (C<sub>2</sub>H<sub>3</sub>O<sup>+</sup>, 43.0178)  
260 saw small contributions from acetone and pentanone, which were subtracted from the acetaldehyde signal. For this  
261 correction, the relative contribution of the fragments from their parent mass, which was determined by the headspace  
262 analysis, was used. A list of the single compounds and their product ions formed in the drift tube can be found in the  
263 supplementary Table S1. Contributions from higher carbonyls in the NO<sup>+</sup> CIMS were not likely since they were not  
264 observed or were below the detection limit.

265

## 266 3 Results

### 267 3.1 Atmospheric conditions and seasonality

268 Seasonality in the central Amazon is characterized by a comparatively less polluted wet season (February–May) and  
269 a more strongly polluted dry season, due to the more frequent influence of biomass burning (August–November)  
270 (Pöhlker et al., 2019; Holanda et al., 2023). The NO<sup>+</sup> CIMS measurements took place from June 23 until July 8 and  
271 from September 27 until October 14, 2019. Below, we outline the meteorological conditions during both measurement  
272 periods as they influenced seasonal variations in observed VOC mixing ratios and correlations. It is important to  
273 consider that the photochemical loss of VOC and reactions involving OH depend on the availability of sunlight, which  
274 also affects the secondary formation of OVOC from the oxidation of different hydrocarbons. VOC emissions from  
275 vegetation are driven by light (photosynthetically active radiation, PAR), temperature, water availability, air pollution,  
276 and biotic factors, such as herbivore infestation, pathogenic infections, or the developmental stage of a plant  
277 (Laothawornkitkul et al., 2009). However, at heights above 80 m, integrated VOC emissions from a whole forested  
278 area domiciled by various plant and herbivorous species at all developmental stages were sampled. As has been  
279 reported previously, inter-seasonal growth variations may even induce the plant to switch from isoprene emission to  
280 monoterpene emission and back (Kuhn et al., 2004a, b). The growth of new leaves (leaf flush), which are  
281 photosynthetically more effective than mature leaves peaks in the dry season and is correlated with the availability of  
282 light (Restrepo-Coupe et al., 2013), which causes an inter-seasonal gradient possibly manifested in the presented  
283 BVOC emissions. The emission and uptake of BVOC by soils and cryptogamic organisms was shown to depend on  
284 the availability of water and could additionally contribute to observed seasonal differences in BVOC concentrations  
285 (Bourtsoukidis et al., 2018; Edtbauer et al., 2021).

286 On average, daytime temperatures differed by only 0.4 °C between the transition (June – July) and the dry season  
287 (Fig. S3). Maximum temperatures in the canopy (at 26 m) were reached at 12:00 local time (LT), with 30.5 °C in the  
288 transition season and 31.2 °C in the dry season on average. The diurnal evolution of temperature closely followed the  
289 incoming solar radiation, here represented by PAR. Dry season observations of PAR were higher by about 9%  
290 compared to the transition season. Precipitation in the month before the NO<sup>+</sup> CIMS measurements took place totaled  
291 157 mm in June and 119 in September 2019 (Fig. S4). The water level measured in the Rio Negro close to Manaus in  
292 2019, however, exhibited maximum values in June and minimum values in October, with a difference of about 10 m  
293 (Chevuturi et al., 2022).

294 The sampled air originated predominantly from the east (SE to NE); thus, an influence from the city of Manaus could  
295 be excluded (Fig. S1). However, for long-lived anthropogenic alkanes, influence from populated areas along the  
296 Amazonas and smaller side rivers was conceivable. The detected alkanes (Table 1) had low mixing ratios below the  
297 detection limit, indicating no significant influence from industries based on fossil fuel combustion.

298 Black carbon (BC) was used as a marker of biomass burning emissions. BC sampled at ATTO has been shown to  
299 originate from biomass burning in South America and Africa (Holanda et al., 2020, 2023). Enhanced concentrations  
300 of 0.42 and 0.54 µg m<sup>-3</sup> (80, 325 m) were found on average in the 2019 dry season. Maximum concentrations reached

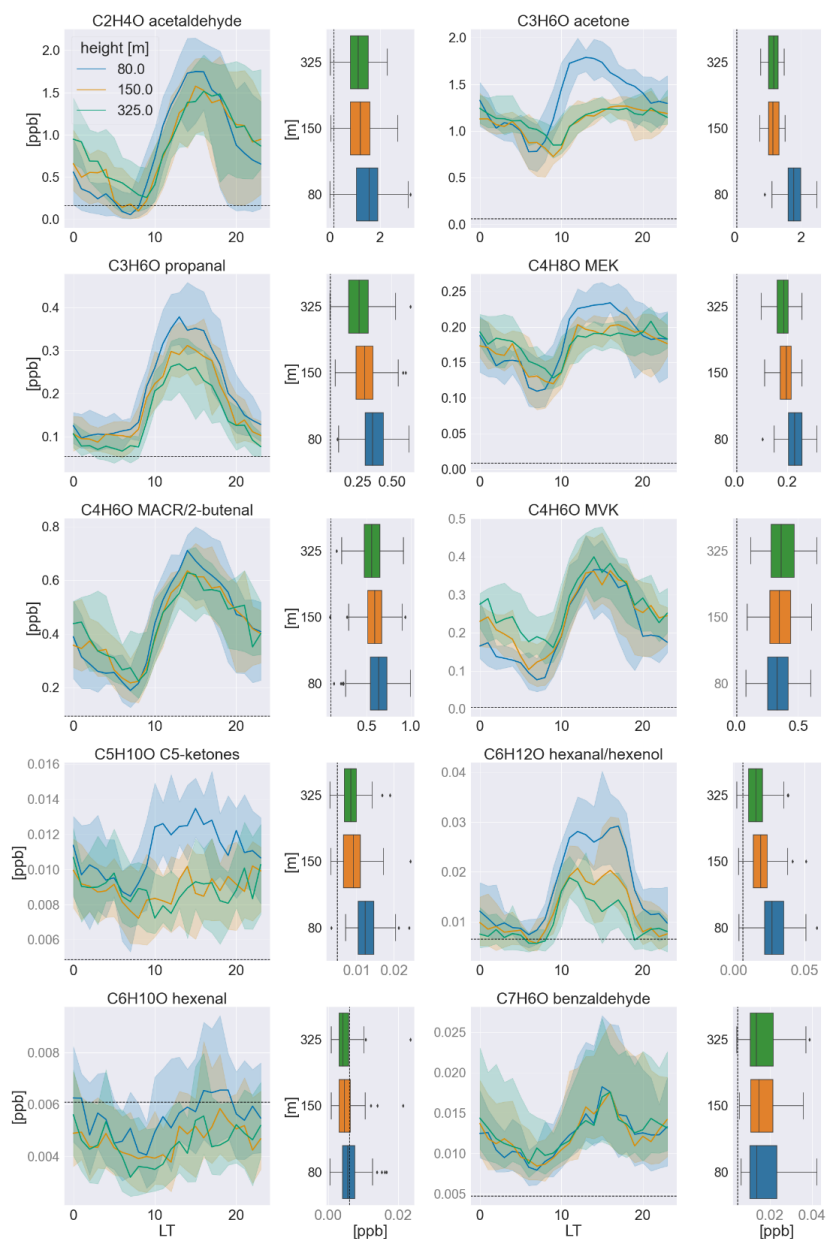


301 0.93 and 1.17  $\mu\text{g m}^{-3}$ . Average concentrations of 0.18 and 0.21 BC (80, 325 m) in the transition season indicated less  
302 polluted conditions. A large number of VOC, including certain carbonyl compounds, are usually co-emitted during  
303 biomass burning with various emission factors and rates (Andreae and Merlet, 2001; Andreae, 2019). Therefore, the  
304 carbonyls detected with the  $\text{NO}^+$  CIMS during this study and their precursors potentially originated from both biogenic  
305 and biomass burning sources. Correlations of carbonyls with BC at 325 m are shown in the Supplementary Data for  
306 both seasons (Fig. S5) to detect possible influences from advected, fresh, or aged biomass burning plumes. In the cases  
307 of acetaldehyde, acetone, methacrolein, MVK, and benzaldehyde, a Pearson coefficient of  $p > 0.55$  was calculated for  
308 the day and nighttime so that an influence of biomass burning through co-advection or in plume production was  
309 feasible.

310

### 311 **3.2 Vertical distribution of carbonyls above the canopy**

312 The distribution of carbonyls with height above the uniform rainforest-covered landscape provides information on the  
313 nature of emission sources, oxidative transformations, and carbonyl sinks under consideration of dynamic processes  
314 in the atmospheric mixed layer. Vertical gradients were governed by the strength and temporal variance of the  
315 respective source, the atmospheric lifetime of the species considered, and dilution through turbulent mixing or  
316 entrainment from the free troposphere during mixed layer growth. Earlier work investigated the chemical and dilutive  
317 loss of isoprene with height using observations at ATTO and a turbulence-resolving large eddy simulation (DALES).  
318 It was shown that slightly more than 50% of the isoprene loss in the vertical (80–325 m) at noon occurred due to  
319 dilutive turbulent mixing (Ringsdorf et al., 2023). It is important to note that the lowest sampling height at 80 m was  
320 within the roughness sublayer. This is a layer within the mixed ABL of about 2–3 times the canopy height ( $\approx 35$  m),  
321 which is strongly affected by the tall canopy with respect to wind fields and, thus, turbulence. Within this layer, the  
322 exchange between the canopy and atmosphere occurs by inhomogeneous flows into and out of the canopy (Chamecki  
323 et al., 2020). An important process influencing the ambient concentration of the compounds presented at all sampling  
324 heights was the growth of the ABL (up to 2 km height) after sunrise due to the strengthening of turbulences from  
325 thermal expansion of the heated air masses near the ground. During ABL growth, air from higher altitudes (residual



326

**Figure 1: Median averaged timeseries in the wet-to-dry transition season (June/July) of 2019 measured at all sampling heights for each carbonyl compound and its respective vertical profile at noon (12:00–15:00 LT) to the right. The shadings indicate the quartiles (25<sup>th</sup> and 75<sup>th</sup>). In the box-and-whisker plots, the boxes also represent the quartiles, while the residual data except for outliers are included in the whiskers. The detection limit (3 sigma) is indicated by dashed, black lines. The mixing ratios in black font were calibrated to a standard, while those in gray font were calculated based on the k-rate.**

327



328 layer containing more chemically aged air) is entrained, leading to the minimum mixing ratios observed after 06:00 LT  
329 at all three heights. During the day, turbulent mixing via convection and associated downward motions is strongest  
330 until convection eases with decreasing insolation. At night, a stable stratification associated with low vertical mixing  
331 is formed (Jordi Vilà-Guerau de Arellano, et al., 2015).

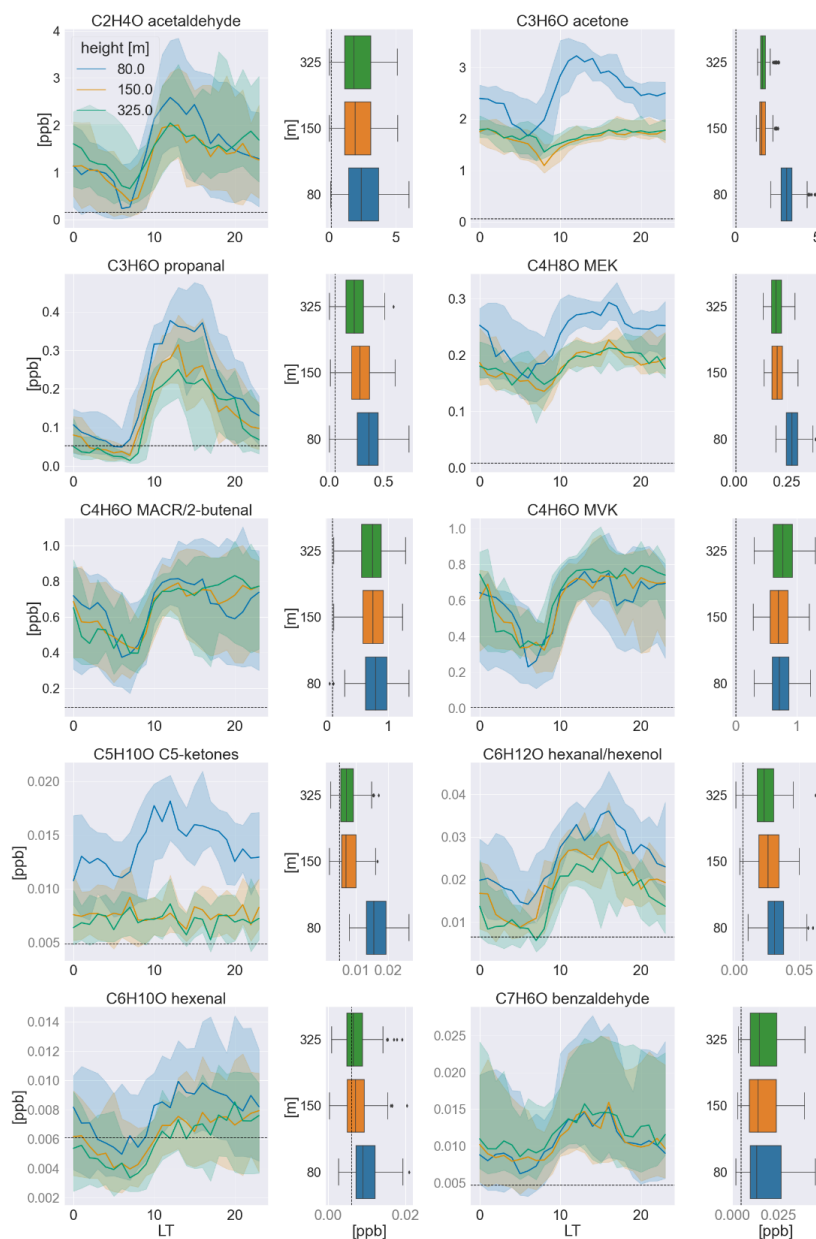
332 Under the reasonable assumption of a carbonyl source at canopy level (based on emission inventories discussed in  
333 Chapter 4), the long-lived ketones were expected to have a background concentration in the convective mixing layer  
334 but also above, while levels of short-lived aldehydes will tend to be zero at higher altitudes, like for isoprene.  
335 Consequently, the aldehydes should show a stronger decrease in their vertical profiles than the ketones, which were  
336 expected to be well-mixed at about a hundred meters above the canopy throughout the convective mixing layer.  
337 Nonetheless, one has to also take the secondary chemical formation of carbonyls into account, which can influence  
338 the vertical gradients depending on the emission source and atmospheric lifetime of the precursors.

339 Figures 1 and 2 present the diurnal cycle observed at the three sampling heights for all carbonyls measured in the wet-  
340 to-dry transition and the dry season, respectively. Some compounds were measured in very low concentrations, below  
341 the detection limit in one or both seasons, namely, the sum of C<sub>5</sub>-aldehydes, C<sub>6</sub>-ketones, heptanal, octanal, and  
342 nonanal. All other carbonyls showed distinct diurnal variabilities with increasing concentrations after sunrise  
343 (06:00 LT) and decreasing concentrations at nighttime. Their diurnal cycle followed the evolution of PAR and  
344 temperature with a slight delay throughout the day, reflecting the expected biogenic emission and photochemical  
345 production. As hypothesized above, no significant vertical variability was found for ketones, though only at 150 and  
346 325 m, whereas a strong decrease in mixing ratio with height was observed between 80 and 150 m. This distribution  
347 indicates that mixing ratios of ketones were only well-mixed above 150 m, while the measurements at 80 m were  
348 influenced by a strong source of ketones, which is discussed compound-wise below. The observed aldehydes exhibited  
349 different vertical distributions; some showed increasing mixing ratios with height, others were rather steadily  
350 decreasing as it was hypothesized, and some showed very small variabilities throughout the lowermost 325 m of the  
351 atmosphere.

352

### 353 **3.3 Correlations at 80m and common sources**

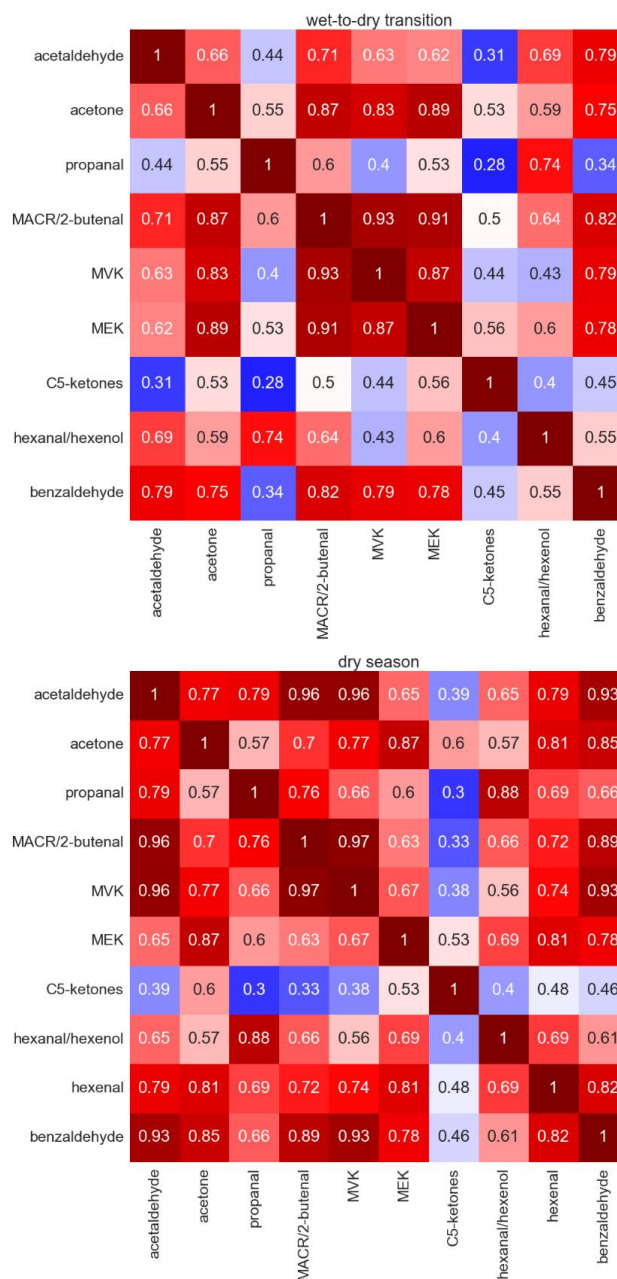
354 The chemical composition of airmasses measured at 80 m was governed by various processes occurring from the leaf  
355 level up to mixing scales of the lower atmosphere. At the leaf level, BVOC are formed by plant metabolic pathways  
356 or, possibly, in the case of OVOC, including carbonyls via within-leaf reactions. Epicuticular waxes, also called leaf  
357 waxes, consist of long-chained hydrocarbons, e.g., the triterpene squalene, which yield OVOC during ozonolysis.  
358 Depending on the position of the double bond of the long-chained molecule and its functional groups, aldehydes or  
359 ketones are formed, whereby the chances for the formation of short-chained carbonyls like acetone are highest  
360 (Fruekilde et al., 1998). Following their emission, a fraction is deposited on surfaces, which is in most cases reversible,  
361 or taken up by stomata, which represents a potential sink (Niinemets et al., 2014). Depending on their atmospheric  
362 lifetime, BVOC undergo within-canopy oxidation; in the case of reactive isoprene and monoterpenes, this was found  
363 to come to not more than 10% of their initial emission flux (Karl et al., 2004; Fuentes et al., 2022) before being ejected  
364 from the canopy. Within and above the canopy they are mixed



365

366

**Figure 2: Median averaged timeseries in the dry season (September/October) of 2019 measured at all sampling heights for each carbonyl compound and its respective vertical profile at noon (12:00–15:00 LT) to the right. The shadings indicate the quartiles (25<sup>th</sup> and 75<sup>th</sup>). In the box-and-whisker plots, the boxes also represent the quartiles, while the residual data except for outliers are included in the whiskers. The detection limit (3 sigma) is indicated by dashed, black lines. The mixing ratios in black font were calibrated to a standard, while those in gray font were calculated based on the k-rate.**



367

**Figure 3: Pearson correlation coefficients for the intercorrelation of carbonyl species in the wet-to-dry transition season (upper) and in the dry season (lower).**

368

369

air masses of varying ages and secondary production and depletion take place simultaneously. When correlating two time series of BVOC measured at that height, a high correlation coefficient can indicate similar production and loss



370 or possibly a precursor–product relationship. Here, it is very important to consider the timescales of production and  
371 loss versus vertical transport since the residence time of air masses in the first 80 m is limited during daytime  
372 convective conditions. In a previous study, the mixing timescale, which accounted for turbulent up and downward  
373 motions between 80 and 325 m at ATTO, was determined to range on average from 60 minutes at 10:00 LT to 15 min  
374 at 15:00 LT (Ringsdorf et al., 2023). Based on that study, we assumed the mean residence time between the canopy  
375 and 80 m to be in the same time range of minutes to 1 hour. Carbonyl precursors including alkenes, isoprene, higher  
376 terpenes, and alkanes have atmospheric lifetimes with respect to oxidation by OH radicals of  $\tau > 2$  hours,  $\tau \approx 3$  hours,  
377 minutes to hours, and days to weeks for the much less reactive alkanes (Altshuler, 1991; Wolfe et al., 2011). The  
378 lifetimes with respect to OH of carbonyl compounds themselves range from 12 hours (trans-3-hexenal) (Jiménez et  
379 al., 2007) to 119 days (acetone) and are even shorter when considering photolysis, which is a significant sink for  
380 carbonyls (Mellouki et al., 2015). In Table 2, the lifetimes of carbonyls with respect to an average OH concentration  
381 of  $1 \times 10^6$  molecules  $\text{cm}^{-3}$  based on a previous study at the ATTO site are presented. This is the average over roughly  
382 the same time of day that was considered for carbonyl correlations (10:00–15:00) (Ringsdorf et al., 2023). However,  
383 isoprene oxidation was observed by the daily increase of the product MVK between 80 and 325 m.

384 Thus, correlations at 80 m will reflect only the processes that occur on a comparable or faster timescale than mixing.  
385 This includes primary emissions, product formation in the atmosphere from short-lived precursors like alkenes and  
386 terpenes, and progressive photochemical degradation/photolysis of short-lived carbonyls as well as loss via deposition.

387 Figures 3–4 show the Pearson correlation coefficients ( $\rho$ ) for both seasons divided into day (10:00–17:00 LT) and  
388 nighttime (22:00–05:00 LT) between the carbonyl compounds and between carbonyls and other selected VOC,  
389 including terpenes (isoprene, sum of monoterpenes), alkenes ( $\text{C}_5$ -alkenes, benzene), and oxygenated compounds  
390 (ethanol, furan, acetic acid,  $\text{C}_5\text{H}_4\text{O}_3$ ). Their diel and vertical distributions are presented in the supplementary figures  
391 S6–S7.  $\text{C}_5\text{H}_4\text{O}_3$  is a highly oxygenated compound, which was classified to be exclusively an oxidation product of very  
392 reactive BVOC in a previous study conducted within and above a pine forest. Therein, emission rates of very reactive  
393 BVOC were estimated to reach 6–30 times the emission rates of monoterpenes (Holzinger et al., 2005). In this study,  
394 the highest mixing ratios were found at 325 m, suggesting that besides being formed as a first-order oxidation product  
395 close to the canopy it was also a higher-order oxidation product that therefore emerges at longer timescales. Very  
396 reactive BVOC presumably also represent precursors for carbonyl compounds. Periods with precipitation were  
397 excluded from the correlations to avoid the effects of downbursts and washout. As expected, high correlations were  
398 found between isoprene and the sum of monoterpenes, which are all primary emissions that depend strongly on light  
399 and temperature. Correlation of carbonyl compounds with isoprene and monoterpenes was preferred over PAR and  
400 temperature to identify light- and temperature-dependent direct emission, due to the temporal delay between emission  
401 and detection. However, it is striking that most carbonyls showed significant correlations with all other carbonyls with



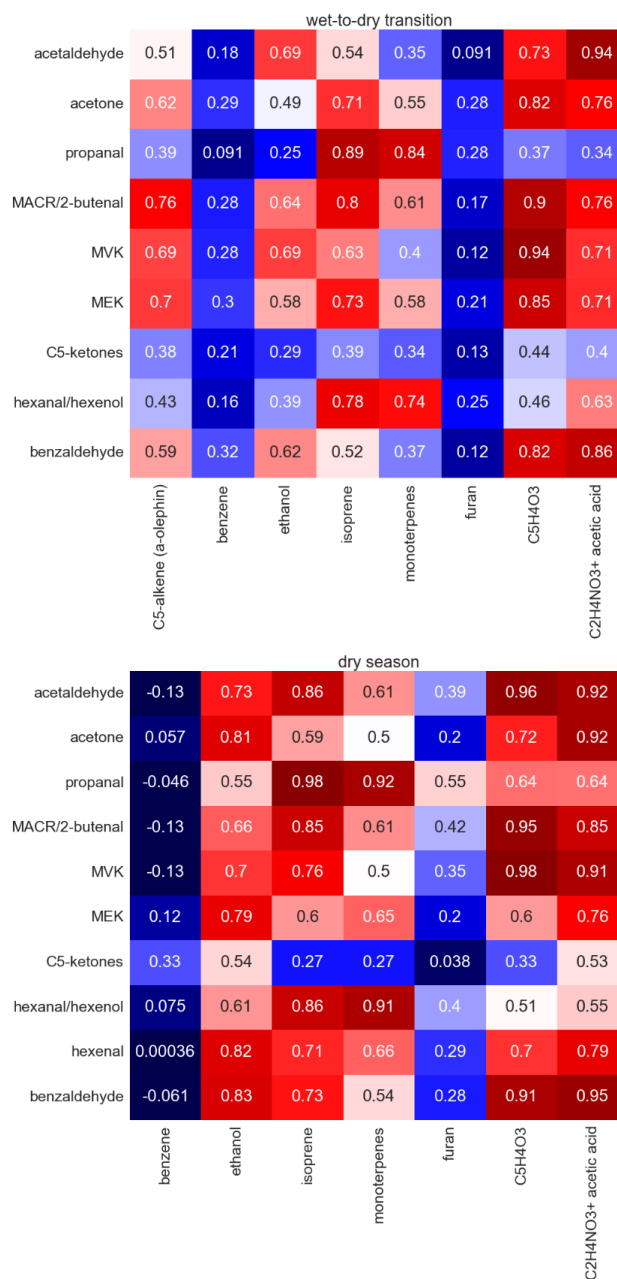


Figure 4: Pearson correlation coefficients for the correlation of carbonyl species with selected hydrocarbons in the wet-to-dry transition season (upper) and the dry season (lower).

402 Pearson coefficients greater than 0.7. This likely resulted from the common driving variables, namely light and  
 403 temperature for emission, as well as similar photochemical production rates.



404 The highest correlations with the primary emitted isoprene and monoterpenes were obtained for propanal and  
405 hexanal. Other compounds that were found to correlate very well were acetaldehyde, methacrolein, MVK, and C<sub>5</sub>H<sub>4</sub>O<sub>3</sub>  
406 as well as acetone and MEK.

### 407 **3.4 Nocturnal loss rates**

408 Biogenic emissions unrelated to photosynthesis might have continued during the night, whereas oxidative chemistry  
409 and, thus, secondary production of carbonyls was limited to reactions with O<sub>3</sub> and NO<sub>3</sub>, which were found at low  
410 levels in the remote forested atmosphere. Important loss mechanisms at night are deposition to surfaces and reaction  
411 with NO<sub>3</sub> (Brown and Stutz, 2012). Deposition at night is thought to happen via adsorption to the cuticle of the leaves,  
412 since stomata are closed in the absence of light. However, there is evidence that the stomatal conductance is maintained  
413 at night by many woody species, implying an irreversible uptake for BVOCs that can be further processed and  
414 converted to other metabolites (Niinemets et al., 2014). Reaction with NO<sub>3</sub> at nighttime is limited to unsaturated  
415 BVOC but is also efficient for some saturated aldehydes. Assuming a rather high mixing ratio of 10 ppt NO<sub>3</sub> (Brown  
416 and Stutz, 2012; Khan et al., 2015), nighttime atmospheric lifetimes of 8 days are estimated for n-hexanal, the most  
417 reactive observed aldehyde with respect to NO<sub>3</sub>. Ozone is circa 1000 times more abundant than NO<sub>3</sub>, but the reaction  
418 rates with carbonyls are much lower. Therefore, deposition is expected to be the dominant loss mechanism for  
419 carbonyls at night. Table 2 summarizes properties of the observed carbonyl compounds that are important driving  
420 variables of deposition on surfaces together with their observed loss rates during the night. These rates were obtained  
421 by linear regression of the observed nocturnal time series at 80 m between 22:00 and 04:00 LT. Since the uptake of  
422 BVOC by leaves occurs only when the ambient concentration exceeds the concentration in the inter-leaf space, high  
423 loss rates were observed for BVOC with high ambient mixing ratios. However, the concentration gradient can be  
424 maintained by a metabolic transformation of the BVOC in the leaf. Table 2 also includes the reactivity of BVOC  
425 towards the OH radical, O<sub>3</sub>, and NO<sub>3</sub>.

426

## 427 **4 Discussion**

428 In the following sections, the diel variability, vertical distribution (80–325 m), and correlations between all measured  
429 BVOC are considered in a compound-wise manner. The measurements presented here are related to previous studies  
430 on the emission, formation, and loss of the carbonyl species.

### 431 **4.1 Acetaldehyde**

432 Acetaldehyde (ethanal) is known to be an important contributor to the total ambient carbonyl concentration in the  
433 atmosphere. Various sources of acetaldehyde have been characterized previously, including direct emissions from  
434 vegetation and the ocean and secondary production from the OH-, NO<sub>3</sub>-, and O<sub>3</sub>-initiated photooxidation of  
435 hydrocarbons (Rottenberger et al., 2004; Wang et al., 2020b). Direct biogenic emissions may be of special importance  
436 for the Amazonian rainforest, as acetaldehyde and ethanol release have been reported to result from root anoxia  
437 (Bracho-Nunez et al., 2012; Holzinger et al., 2000; Rottenberger et al., 2008). This may occur in large areas caused



**Table 2: Rate coefficients for the reaction with OH, NO<sub>3</sub>, and O<sub>3</sub> and the atmospheric lifetime considering an OH radical concentration of 1x10<sup>6</sup> molecules cm<sup>-1</sup>. The rate coefficients and boiling point temperature were taken from the NIST database. Water solubility has been reported by Sander et al., 2023. The loss rate is calculated based on the median averaged slopes of the nocturnal (22:00–04:00) carbonyl timeseries.**

| VOC species                              | k <sub>OH</sub><br>[cm <sup>3</sup> # <sup>-1</sup> s <sup>-1</sup> ] | Estimated<br>lifetime Amazon<br>[days] | k <sub>NO<sub>3</sub></sub><br>[cm <sup>3</sup> # <sup>-1</sup> s <sup>-1</sup> ] | k <sub>O<sub>3</sub></sub><br>[cm <sup>3</sup> # <sup>-1</sup> s <sup>-1</sup> ] | Volatility<br>(T <sub>boil</sub> [K]) | Water-<br>solubility (H <sub>s</sub> <sup>CP</sup> )<br>[mol m <sup>-3</sup> Pa <sup>-1</sup> ] | Loss rate<br>[ppb min <sup>-1</sup> ]<br>(transition, dry<br>season) |
|--|---|--|---|--|---------------------------------------|---|--|
| Acetaldehyde                             | 1.6E-11   | 1.4                                    | 2.4E-15   | 3.4E-20  | 294                                   | 1.3E-1  | -6.7E-4,<br>-1E-3  |
| Acetone                                  | 1.9E-13   | 119.3                                  | 8.5E-18   | 8.5E-18  | 329                                   | 2.7E-1  | -7.8E-4,<br>-9.5E-4  |
| Propanal                                 | 2E-11   | 1.2                                    | 6.2E-15   | -  | 322                                   | 9.9E-2  | -8.9E-5,<br>-1.4E-4  |
| MEK                                      | 1.2E-12   | 19.3                                   | -   | 2.06E-16   | 353                                   | 1.8E-1  | -8.4E-5,<br>-7.4E-5  |
| MVK                                      | 1.9E-11   | 1.25                                   | 1.2E-16   | 4.48E-18   | 354                                   | 4.0E-1  | -1.1E-4,<br>-4.8E-4  |
| MACR                                     | 3E-11   | 0.75                                   | 3.3E-15   | 1.09E-18   | 341                                   | 4.5E-2  | -2.1E-4,   |
| 2-Butenal                                | 3.6E-11   | 0.64                                   | 5.1E-15   | 1.58E-18   | 375.5                                 | 5.9E-1  | -2.1E-4  |
| 2-pentanone<br>(C <sub>5</sub> -ketones) | 4.6E-12   | 5.08                                   | -   | -  | 375                                   | 1.3E-1  | -  |
| n-hexanal                                | 2.8E-11   | 0.83                                   | 1.1E-14   | -  | 402                                   | 4.5E-2  | -2E-6  |
| Z-3-hexenal                              | 1E-10   | 0.21                                   | 2.7E-13   | 6.4E-17  | 427.7                                 | -   | -  |
| z-2-hexenal                              | 4.4E-11   | 0.52                                   | 1.2E-14   | 2.0E-18  | 419.7                                 | 1.4E-1  | -  |
| Benzaldehyde                             | 1.3E-11   | 1.78                                   | 2.01E-15  | 2.0E-19  | 452                                   | 4.0E-1  | -7.9E-6,<br>-8E-6  |
| Isoprene                                 | 1E-10   | 0.23                                   | 6.7E-13   | 1.28E-17   | 307                                   | 1.3E-4  | -1.5E-3,<br>-2.6E-3  |
| α-pinene                                 | 5.3E-11   | 0.43                                   | 6.2E-12   | 9.6E-17  | 430                                   | 7E-4  | 1.7E-4,<br>-3.2E-4   |

438 by seasonal flooding (Parolin et al., 2004). At 80, 150, and 325 m in the wet-to-dry transition season of 2019, observed  
439 mean diurnal concentrations were 642, 702, 852 ppt, respectively, and 1.38, 1.25, 1.47 ppb in the dry season of 2019.

440 Metabolic production pathways of acetaldehyde within plants and subsequent emission have been found to occur not  
441 only during root-flooding but also during rapid light-dark transitions (Fall, 2003; Holzinger et al., 2000). The anaerobic  
442 conditions at the root's surface during flooding cause the ethanolic fermentation pathway to form ethanol that is  
443 transported to the leaves of the plant to provide an energy source.

444 Acetaldehyde is an intermediate of this pathway which tends to leak out to the atmosphere due to its high volatility  
445 (Kreuzwieser et al., 2000). Some Amazonian tree species can switch to fermentative metabolism (Bracho-Nunez et  
446 al., 2012), but concentration or flux measurements during the dry-to-wet transition in Amazonia under field  
447 conditions are missing. In this study, a strong correlation was found for ethanol and acetaldehyde in the nighttime  
448 during the transition season (p = 0.92). Ethanol mixing ratios were ten times higher in the transition season and showed  
449 a diel maximum at nighttime. Since river levels were at their maximum levels in the transition season, root flooding



**Table 3: Median averaged mixing ratios of the observed carbonyl compounds for the measurement periods in the dry-to-wet transition and the 2019 dry season. The range presents the lowest mixing ratio included in the 25<sup>th</sup> and the highest mixing ratio included in the 75<sup>th</sup> quantile of the median averaged diurnal cycle. Numbers in italics represent the limit of detection.**

| Carbonyl species        | Height [m] | Wet-to-dry transition – Jun-Jul 2019 |             | Dry season 2019 – Sep-Oct 2019 |                   |
|-------------------------|------------|--------------------------------------|-------------|--------------------------------|-------------------|
|                         |            | Median [ppt]                         | Range [ppt] | Median [ppt]                   | Range [ppt]       |
| Acetaldehyde            | 80         | 642                                  | 24 - 2043   | 1380                           | <i>160</i> - 3179 |
|                         | 150        | 702                                  | 24 - 1801   | 1252                           | 239 - 3134        |
|                         | 325        | 852                                  | 59 - 1883   | 1472                           | 256 - 3716        |
| Acetone                 | 80         | 1333                                 | 559 - 2083  | 2546                           | 1155 - 3812       |
|                         | 150        | 1124                                 | 494 - 1509  | 1657                           | 918 - 2105        |
|                         | 325        | 1146                                 | 661 - 1545  | 1707                           | 1087 - 2115       |
| Propanal                | 80         | 176                                  | 71 - 438    | 165                            | 53 - 410          |
|                         | 150        | 150                                  | 58 - 365    | 115                            | 53 - 349          |
|                         | 325        | 119                                  | 53 - 348    | 85                             | 53 - 305          |
| MEK                     | 80         | 177                                  | 82 - 267    | 249                            | 116 - 348         |
|                         | 150        | 175                                  | 81 - 229    | 188                            | 98 - 259          |
|                         | 325        | 177                                  | 105 - 240   | 185                            | 75 - 247          |
| MVK                     | 80         | 184                                  | 45 - 483    | 607                            | 100 - 994         |
|                         | 150        | 229                                  | 53 - 481    | 599                            | 164 - 967         |
|                         | 325        | 265                                  | 93 - 499    | 659                            | 239 - 1014        |
| MACR/2-Butenal          | 80         | 415                                  | 149 - 755   | 679                            | 250 - 1026        |
|                         | 150        | 425                                  | 149 - 697   | 644                            | 307 - 1010        |
|                         | 325        | 439                                  | 181 - 694   | 644                            | 281 - 996         |
| C <sub>5</sub> -ketones | 80         | 11                                   | 7 - 18      | 14                             | 7 - 23            |
|                         | 150        | 9                                    | 7 - 15      | 8                              | 7 - 13            |
|                         | 325        | 9                                    | 7 - 15      | 7                              | 7 - 12            |
| n-hexanal/ hexenols     | 80         | 15                                   | 6 - 50      | 26                             | 6 - 53            |
|                         | 150        | 11                                   | 6 - 33      | 19                             | 6 - 42            |
|                         | 325        | 9                                    | 6 - 30      | 16                             | 6 - 43            |
| z-2-hexenal             | 80         | -                                    | < 11        | 8                              | 6 - 14            |
|                         | 150        | -                                    | < 9         | -                              | < 12              |
|                         | 325        | -                                    | < 9         | -                              | < 12              |
| Benzaldehyde            | 80         | 12                                   | 6 - 27      | 11                             | 6 - 26            |
|                         | 150        | 12                                   | 6 - 24      | 10                             | 6 - 26            |
|                         | 325        | 12                                   | 6 - 24      | 11                             | 6 - 25            |

450 may be responsible for the seasonal variability of ethanol (Kirstine and Galbally, 2012). However, acetaldehyde  
 451 showed a different seasonal variability, indicating other sources were dominant. It is important to keep in mind that  
 452 the ATTO site is a “Terra firme” region with inundation events rare. Field measurements of roots under anoxia are  
 453 still missing. Fast light–dark transitions occur continuously inside the forest canopy and are suspected to lead to an  
 454 overproduction of cytosolic pyruvic acid in the leaves that is converted to acetaldehyde as a safety mechanism against  
 455 acidification (Fall, 2003). The wounding of a plant through cutting or drying out of plant tissues also leads to release  
 456 of acetaldehyde (Guenther, 2000). The compound is also found in emissions from leaf litter presumably as a byproduct  
 457 of biomass degradation (Schade and Goldstein, 2001; Karl et al., 2003). Furthermore, the oxidation of polyunsaturated  
 458 fatty acids in leaves leads to the formation of reactive aldehydes, which can represent a primary source for many  
 459 aldehydes, including acetaldehyde (Niinemets et al., 2014; Matsui et al., 2010). Once released, the atmospheric  
 460 lifetime of acetaldehyde is in the range of 1.4 days with respect to OH (Table 2).



461 Tree branch enclosures and vertical gradient measurements at another Amazonian measurement site (Rondônia) in  
462 1999 revealed that the canopy's role as a sink can even exceed its function in emissions. Uptake to leaves mainly  
463 occurred via the leaf stomata and has been reported to be governed by a compensation point that varies between  
464 canopy and understory species. The authors concluded that the observed ambient concentrations were generated  
465 mainly by the secondary photochemical production of acetaldehyde (Rottenberger et al., 2004). Accordingly, in 2013,  
466 measurements of acetaldehyde vertical gradients below 80 m at ATTO showed increasing acetaldehyde between 24 m  
467 (inside the canopy, high influence by surrounding trees) and 79 m. However, interestingly, this has only been observed  
468 in the dry season (Sep), whereas during the wet season of 2013 (Feb/Mar), a dominance of primary emission over  
469 secondary production was indicated by decreasing concentrations directly above the canopy (Yáñez-Serrano et al.,  
470 2015). We observed decreasing mixing ratios at altitudes above 80 m under dry season or close to dry season  
471 conditions in 2019. At noon, the acetaldehyde mixing ratios peaked in the first 150 m above the canopy, consistent  
472 with a rapid secondary production and a possible contribution from direct emission. Primary emission might vary in  
473 strength and dominance with season due to the variability of light, temperature, precipitation, and soil moisture and  
474 due to plant phenology. At 150 and 325 m, similar mixing ratios were measured, suggesting well-mixed conditions  
475 and ongoing secondary formation between those heights, due to the many routes of acetaldehyde photochemical  
476 generation.

477 In the rainforest environment, sources of the photochemical precursor hydrocarbons of acetaldehyde are most likely  
478 to be natural emissions or longer-lived emissions from distant biomass burning. Aldehydes are a common product of  
479 any hydrocarbons that are oxidized in the atmosphere (Mellouki et al., 2015; Calogirou et al., 1999). Laboratory  
480 experiments showed that acetaldehyde emerges from the oxidation of alkanes and alkenes, with ethane and propene  
481 having the largest emission fluxes globally (Singh et al., 2004). Ethane is globally distributed; thus, background  
482 concentrations of acetaldehyde are generated by this route, which are, however, low due to the rapid subsequent  
483 transformation via reaction with OH. Biogenically emitted compounds with high molar yields for the formation of  
484 acetaldehyde are  $> C_2$  alkenes (0.85) and ethanol (0.95). Additionally, isoprene and terpenes have a low molar yield  
485 (0.019, 0.025) but exhibit the strongest emissions measured from the forest (Fischer et al., 2014). The reaction of other  
486 aldehydes butanal, 2-pentanone, and 2-heptanone with OH and  $NO_3$  also leads to the formation of acetaldehyde,  
487 sometimes with high yields (Atkinson et al., 2000). In the data presented here, acetaldehyde at 80 m correlated best  
488 with photolytically generated species like MVK, methacrolein, and  $C_5H_4O_3$  ( $p = 0.96$ ) and with benzaldehyde  
489 ( $p = 0.93$ ) in the dry season and correlated well with acetic acid ( $p > 0.92$ ) in both seasons. In the transition season  
490 correlations were weaker overall (Figs. 3–4), which could hint at different primary and secondary acetaldehyde  
491 sources. Correlation coefficients of acetaldehyde and BC at 325 m were below 0.6 at daytime but at nighttime, in the  
492 transition season, a rather high correlation with  $p = 0.82$  was observed (Fig. S6).

493 From about 16:00 LT onwards until the next day the vertical gradient is reversed with the lowest concentrations at  
494 80 m. This likely reflects the uptake to plant tissues regulated by compensation points since the  $NO_3$  and  $O_3$  reactivity  
495 is rather low. Acetaldehyde exhibits the strongest observed loss rate at nighttime among all the carbonyl compounds  
496 in the dry season and it had the highest Henry's law constant (Table 2).

#### 497 **4.2 Acetone**

498 Acetone (propanone) is the simplest ketone and the most abundant and widespread OVOC in the atmosphere due to  
499 its relatively long atmospheric lifetime of 15 days (Singh et al., 2004) (primarily driven by photolysis in the upper  
500 troposphere, 119 days with respect to OH). The variation of acetone mixing ratios throughout the day above the  
501 roughness sublayer at 150 and 325 m was small compared to the other carbonyls. However, mixing ratios at 80 m  
502 increased substantially with light and temperature during the day. In the wet-to-dry transition season mixing ratios  
503 reached 1.33, 1.12, 1.15 ppb on average, while in the dry season, 2.55, 1.66, 1.71 ppb (80, 150, 325 m) were measured.

504 The vertical distribution of acetone showed clearly enhanced mixing ratios at 80 m during daytime compared to well-  
505 mixed conditions at higher altitudes. The strong gradient in the first 150 m above the canopy indicated a large positive  
506 flux above the canopy. Possible reasons for this strong gradient include primary biogenic emission, biomass burning,  
507 production from leaf wax, or efficient secondary formation from very short-lived precursors that exceed deposition  
508 and stomatal uptake. Flux measurements in a tropical forest in Costa Rica in the dry season have found a bidirectional  
509 but net-positive canopy flux of acetone (Karl et al., 2004). Additionally in 2013, when several carbonyls were



510 measured at ATTO below 80 m, the acetone mixing ratios inside the canopy (influenced by surrounding trees) were  
511 lower than the values measured at 79 m in the dry season. As for acetaldehyde, these increasing vertical gradients  
512 suggested a dominance of photolytically secondary formation over direct emission. In the wet season in 2013,  
513 however, mixing ratios measured in the canopy and at 79 m were of similar magnitude and, compared to the dry  
514 season, much lower at both heights. In conclusion, no clear dominance of secondary formation or direct emission was  
515 found in the wet season (Yáñez-Serrano et al., 2015). We also observed seasonal differences at all three heights, with  
516 lower mixing ratios in the transition compared to the dry season. While we cannot report acetone observations from  
517 the wet season, we did observe higher correlations of acetone with non-primary emitted OVOC methacrolein, MVK,  
518 and  $C_3H_4O_3$  in the transition season ( $p > 0.82$ ) compared to the dry season, suggesting that in 2019 secondary  
519 formation contributed more acetone to observed mixing ratios in the transition season than in the dry season. In light  
520 of the widely differing atmospheric lifetimes of acetone and those OVOC, the most likely explanation for the high  
521 transition season correlations is a dominating secondary acetone source at a similar rate. Contributions from aged  
522 biomass burning plumes containing acetone in the dry season, when enhanced BC concentrations were observed,  
523 could also be the reason for a weaker correlation of  $C_3H_4O_3$ , methacrolein, and MVK with acetone in the dry season.  
524 Based on the information obtained in 2013 and the data from this study, secondary production in the dry and transition  
525 season appears to peak between the canopy and 150 m above ground, adding up to varying contributions of direct  
526 emissions from vegetation. In conclusion, the most relevant precursors were very reactive biogenic compounds. The  
527 best correlations were found with MEK ( $p > 0.87$ ) in both seasons, which is another long-lived ketone that is known  
528 to be directly emitted from the Amazon rainforest and produced in the atmosphere overhead (Yáñez-Serrano et al.,  
529 2015, 2016).

530 Primary sources of acetone are direct emission from vegetation and, to a smaller extent, also from dead plant matter.  
531 Acetone is released during cyanogenesis, which acts as a repellent that stops herbivores eating the plant's leaves.  
532 During the production and release of volatile hydrogen cyanide, which deters the feeding herbivore, acetone is formed  
533 as a byproduct. Cyanogenesis occurs in many plant species, though some employ different mechanisms to produce  
534 hydrogen cyanide so that other carbonyl byproducts can be released (Fall, 2003). Another known biogenic pathway  
535 for acetone formation is acetoacetate decarboxylation in soil bacteria and humans (Fall, 2003). Both light and  
536 temperature have been suspected to drive acetone emissions, as shown for some pine and spruce trees (Seco et al.,  
537 2007).

538 Secondary formation of acetone is known to occur from anthropogenically emitted  $C_3$ - $C_5$  isoalkanes (propane,  
539 isobutane, isopentane) and biogenic emitted methyl butenol and certain terpenes (Seco et al., 2007; Fischer et al.,  
540 2014; Jacob et al., 2002). We found mixing ratios of isopentane to be below the detection limit (13 ppt), and the  
541 vertical distribution and correlations reported for acetone indicated a rapid formation in the first 150 m above ground  
542 by hydrocarbons that are much more short-lived than alkanes.

543 At night, deposition could be observed on the basis of the rapidly decreasing mixing ratios at 80 m, compared to the  
544 slowly occurring reactions with  $NO_3$  and  $O_3$ . Similar effects have been reported in flux measurements performed by  
545 Karl et al. (2004).

### 546 **4.3 Propanal**

547 Propanal is an isomer of acetone and is not distinguishable from acetone by classical PTR-MS type instruments using  
548  $H_3O^+$ . In this study, the first high temporal resolution measurements of propanal in a tropical forest are presented, and  
549 the vertical distribution above the canopy was found to differ markedly from acetone. In general, in the remote  
550 atmosphere, we may expect the more reactive propanal to have lower mixing ratios than acetone, although this may  
551 not be true close to sources. We measured average concentrations of 176, 150, and 119 ppt in the wet-to-dry transition  
552 and 165, 115, and 85 ppt in the dry season (80, 150, 325 m). The ratio of propanal to acetone in the roughness sublayer  
553 of the tropical forest and above yields 1:7.6, 1:9.6 (transition season) and 1:15.4, 1:20 (dry season) at 80 and 325 m.  
554 Globally, the mixing ratio of propanal has been estimated to be about one-third of acetaldehyde (Singh et al., 2004),  
555 while at ATTO a ratio of 1:4.2, 1:8.1 (transition season) and 1:7.2, 1:14 (dry season) was measured at 80 and 325 m,  
556 respectively. However, it should be noted that, globally, a large propanal source is propane oxidation, which is  
557 predominantly emitted from anthropogenic activities associated with oil and gas use. Acetaldehyde sources in the  
558 rainforest thus far exceed propanal sources in the context of the global budget (Warneck, P.; Williams, J., 2012).



559 Propanal emission from vegetation has been reported for non-tropical forests (Guenther, 2000; Villanueva-Fierro et al., 2004), although the metabolic pathway was not specified. Wang et al. (2019) described the biosynthesis of acetaldehyde and propanal during fruit ripening. It was also noted that propanal emission occurs from ferns (Isidorov et al., 1985), which is important since fern species are common in the understory of tropical forests.

563 Throughout the day, propanal exhibited a negative vertical gradient (i.e., decreasing mixing ratio with increasing height). This occurs most likely due to dilution and photochemical loss of propanal generated in or emitted from the canopy. A similar distribution was also observed for monoterpenes and isoprene, which are primary emitted VOC. Accordingly, propanal observed at 80 m also correlates best with isoprene in both seasons ( $0.89 > p > 0.98$ ) followed by monoterpenes ( $0.84 > p > 0.92$ ). The estimated atmospheric lifetime of propanal of about 1 day (Guimbaud et al., 2007) (1.2 days for the oxidation by OH, table 2) is similar to that of acetaldehyde, but the vertical profiles revealed different distributions in the first 325 m above ground (Figures 1 and 2). The weak gradient of acetaldehyde between 150 and 325 m at daytime in contrast to the steadily decreasing vertical profile of propanal can thus only be explained by a higher yield of acetaldehyde from secondary production above 150 m. This is not surprising since acetaldehyde is produced during oxidative degradation of many hydrocarbons. The secondary production of propanal is known to occur via the photochemical oxidation of  $C_3$  and larger hydrocarbons (Singh et al., 2004) and propane (Altshuller, 1991). Their lifetimes range from 5 days to a few hours (Altshuller, 1991). However, due to the high correlation of propanal and isoprene, which is even higher than the correlation of isoprene and its oxidation products MVK and methacrolein, a primary and mainly light-dependent source is surmised.

577 Nighttime mixing ratios of propanal were decreasing at 80 m (Table 2). Since the reaction rate of propanal with  $NO_3$  is faster and the water solubility lower than that of the other carbonyl compounds, a higher fraction could potentially react in the atmosphere. Stomatal uptake for the terpenes might be driven by the concentration gradient between leaf and atmosphere, and the same might hold for propanal.

#### 581 **4.4 Methyl Ethyl Ketone (MEK)**

582 Mixing ratios of MEK in the wet-to-dry transition were 177, 175, and 177 ppt on average, compared to 249, 188, and 185 ppb in the dry season (80, 150, 325 m). With a conventional PTR-MS, butanal and MEK are detected at the same exact mass, whereas in this study using  $NO^+$  reagent ions solely MEK was measured. Butanal mixing ratios were determined to be below the detection limit (20 ppt); thus, the contribution of butanal to MEK for PTR-MS can be assumed to be very low. The mixing ratios obtained in this study agree well with previous studies conducted with a PTR-quadrupole-MS at the ATTO site in 2013 and close to Manaus (Amazonia) in 2014, which would not completely exclude possible interferences on the nominal mass of MEK (Yáñez-Serrano et al., 2015, 2016). The vertical distribution of MEK throughout the day resembles that of acetone in both seasons. Mixing ratios above the roughness layer (at 150 and 325 m) were almost uniform, while those at 80 m showed a more pronounced diurnal cycle with strongly increasing values in the day and decreasing values at night. As well as being structurally similar to acetone, MEK also has a long lifetime of 4.3 days (Fischer et al., 2014) (19.3 with respect to OH oxidation alone) relative to mixing timescales. MEK is also known to have primary and secondary sources (Yáñez-Serrano et al., 2016). Therefore, it is not surprising that MEK correlated best with acetone at 80 m ( $p = 0.87$  in the dry season), but in the transition season, it also correlated well with  $C_3H_4O_3$ , methacrolein, and MVK. This suggests secondary sources from biogenically emitted precursors were more dominant during the transition season than in the dry season, similar to acetone.

598 MEK emissions have been reported for rainforest canopies (Yáñez-Serrano et al., 2015) and fern (Isidorov et al., 1985), decaying plant matter (Warneke et al., 1999), fungi, and bacteria (Yáñez-Serrano et al., 2016). The metabolic pathways of production and the release mechanisms are poorly understood but have been suggested to involve plant signaling, injured leaves, and root-aphid interactions (Yáñez-Serrano et al., 2016). Within-plant conversion of the cytotoxic 1,2-ISOPROOH, which was deposited on poplar leaves, first to MVK and subsequently to MEK, has been reported to represent a large biogenic source of MEK. The enzyme responsible for the conversion of MVK to MEK is widespread among plants (Canaval et al., 2020).

605 The secondary formation of MEK occurs via the oxidation of n-butane with a yield of 80% (Singh et al., 2004) and via oxidation of 2-butanol, 3-methyl pentane, and 2-methyl-1-butene (Yáñez-Serrano et al., 2016). Additionally, all





607 alkenes with a methyl/ethyl group on the same side of the olefin bond are possible precursors of MEK (Singh et al.,  
608 2004). Butane was not expected to be abundant in the rainforest environment due to its anthropogenic sources, and  
609 butane oxidation would also yield butanal, which was only detected below the LOD. As for acetone, the vertical  
610 distribution and correlations discussed above suggest higher levels of short-lived precursors of MEK than of alkanes.

611 Rapidly decreasing concentrations at 80 m at night are in agreement with earlier studies, that reported deposition of  
612 MEK in the canopy due to its high water solubility (Yáñez-Serrano et al., 2016) (Table 2).

#### 613 **4.5 Methyl Vinyl Ketone and Methacrolein/2-Butenal**

614 The main source of both carbonyls MVK and methacrolein is the oxidation of isoprene by OH. Thus, they are  
615 summarized in one section. It has been shown previously that methacrolein is detected together with 2-butenal (Koss  
616 et al., 2016), which is also found in vegetation emission studies, albeit in small concentrations (Isidorov et al., 1985;  
617 Hellén et al., 2004). (E)-2-butenal is a signaling compound within the plant that serves to trigger responses to abiotic  
618 stress (Yamauchi et al., 2015). Its atmospheric lifetime is around 20 hours, slightly longer than the lifetimes of  
619 methacrolein and MVK which are 10 and 14 hours, respectively (Hellén et al., 2004; Liu et al., 2016). It is also known  
620 that MVK and methacrolein cannot be detected separately from isoprene hydroxyhydroperoxides (ISOPOOH) without  
621 using a scrubber, since the hydroperoxides decompose onto the same m/z. With NO<sup>+</sup> CIMS the fragment of 1,2-  
622 ISOPOOH and methacrolein share one m/z-ratio, while 4,3-ISOPOOH is detected together with MVK (Rivera-Rios  
623 et al., 2014). Wall exchange effects in the inlet line might have led to the removal of ISOPOOH from the sampled air  
624 due to their reduced volatility, but a contribution to the MVK and methacrolein signal remains possible. ISOPOOH  
625 also originate from the oxidation of isoprene and are very reactive, reflected by lifetimes of 3 and 2 hours. After the  
626 initial reaction of OH and isoprene, the subsequently formed peroxy radical (RO<sub>2</sub>) can react with NO to form MVK  
627 and methacrolein, but it can also react with HO<sub>2</sub> to form ISOPOOH (Liu et al., 2016). At close to pristine conditions  
628 at ATTO, NO mixing ratios are low, and the yield distribution between ISOPOOH, MVK, and methacrolein was  
629 estimated to be 50, 25, and 25%, respectively (Rivera-Rios et al., 2014; Ringsdorf et al., 2023). It has been shown that  
630 the oxidation of isoprene can proceed already within plant tissues by reaction with accumulated reactive oxygen  
631 species. The accumulation of reactive oxygen species, including OH, is a reaction to biotic and abiotic stresses and  
632 can exceed the antioxidant defense capacities in the tissue. The oxidation of isoprene within the tissue reduces the  
633 amount of reactive oxidized species and leads to the direct emission of isoprene's products MVK and methacrolein,  
634 especially under stress (Jardine et al., 2012b, 2013).

635 Oxidation of the monoterpene ocimene has been identified as another secondary source for MVK (Calogirou et al.,  
636 1999). To our knowledge, there are no other significant direct or secondary sources of MVK, methacrolein, and  
637 ISOPOOH other than the oxidation of isoprene. This explains the observed diurnal cycle with an afternoon maximum  
638 due to the light-dependent emission of isoprene and the photochemical production of OH. Since isoprene is present at  
639 relatively high mixing ratios at all tree sampling heights (3.69, 3.33, 3.0 ppb at 80, 150, and 325 m in the dry season),  
640 the oxidative formation of MVK, methacrolein, and ISOPOOH takes place throughout the mixed layer. The observed  
641 slightly increasing mixing ratios of MVK with height are consistent with rapid isoprene oxidation above the canopy,  
642 slower removal of MVK itself, and turbulent in-mixing of cleaner air from above. Isoprene has an estimated  
643 atmospheric lifetime of about 3 hours, and it was previously reported that only circa 10% of emitted isoprene was  
644 oxidized within the canopy (Karl et al., 2004). Unlike MVK, methacrolein and 2-butenal show a slightly decreasing  
645 vertical gradient. Sources and sinks of MVK and methacrolein are very closely related, so the presence of significant  
646 quantities of 2-butenal is the most likely explanation for that difference.

647 Dry deposition to leaf surfaces has been observed in a previous study for the sum of MVK and methacrolein and  
648 individually for these compounds during daytime (Nguyen et al., 2015; Tani et al., 2010). Uptake by leaves represents  
649 a significant sink that exceeds loss via OH oxidation near leaves (Tani et al., 2010). In this study, the rapid decrease  
650 of nocturnal concentrations at 80 m indicated that deposition at night was also taking place.

651 MVK and methacrolein + 2-butenal showed similar mixing ratios in the dry season of 607, 599, 659 ppt MVK and  
652 679, 644, 644 ppt methacrolein + 2-butenal. It has to be considered that the uncertainty of MVK mixing ratios is higher  
653 than the uncertainty of methacrolein mixing ratios due to their k-rate-based calculation rather than calibration to a gas  
654 standard. In the transition season, methacrolein + 2-butenal (415, 425, 439 ppt) exceeded the mixing ratios of MVK



655 (184, 229, 265 ppt). Whether that resulted from the high seasonal variability of 2-butanal or from the contribution of  
656 ISOPOOH, unfortunately, remains unclear. Lower levels of all isoprene oxidation products were expected as a result  
657 of lower isoprene mixing ratios and photo-oxidation rates in the transition season.

#### 658 **4.6 Sum of C<sub>5</sub>-ketones**

659 The mixing ratios obtained for the sum of C<sub>5</sub>-ketones were 11, 9, and 9 ppt in the transition season, while slightly  
660 higher levels of 14, 8, and 7 ppt (80, 150, 325 m) were obtained in the dry season. A diurnal cycle was observed at  
661 80 m only, whereas levels at 150 and 325 m were similar and showed no trend throughout the day and night. C<sub>5</sub>-  
662 ketones were 2- and 3- pentanone as well as 3-methyl-2-butanone. The atmospheric lifetime of 2-pentanone is in the  
663 range of 5 days. All three ketones have been included in emission inventories from plants (Isidorov et al., 1985; König  
664 et al., 1995; Kesselmeier and Staudt, 1999), but there is little information on metabolic pathways or mechanisms. 2-  
665 pentanone has been identified as a marker for fungal activity in indoor environments (Kalalian et al., 2020), since it is  
666 produced in the hyphae of *Aspergillus niger* (Lewis, 1970), a fungus that was also found to degrade biomass in the  
667 Amazon. 3-pentanone is one of the C<sub>5</sub> green leaf volatiles (GLV) emitted at lower rates than C<sub>6</sub> GLV, which are  
668 described in the next section (Jardine et al., 2012a). An increase of 3-pentanone coincident with high temperatures  
669 after noon was observed at another measurement station in the Amazon rainforest, with a simultaneous decrease of  
670 terpenoid emissions (Jardine et al., 2015). Consistent with this observation, in this study, the correlation of C<sub>5</sub> ketones  
671 with isoprene or monoterpenes was low in the transition and dry season during the daytime ( $p < 0.39$ ). The best  
672 correlations for C<sub>5</sub>-ketones of  $0.53 < p < 0.6$  were obtained with acetone and MEK. This was most likely a  
673 consequence of common sources, including primary emission and formation from rather short-lived hydrocarbons and  
674 of the long atmospheric lifetimes relative to mixing timescales, which the observed ketones have in common. Above  
675 150 m, no diurnal variability was observed, which is also in agreement with the other ketones, suggesting they were  
676 well-mixed above the Amazonian roughness sublayer.

677 Fumigation experiments with different VOC have shown a loss of all three C<sub>5</sub>-ketones on leaf surfaces (Tani and  
678 Hewitt, 2009). A decrease of the mixing ratios at 80 m could be observed at nighttime, and a high water solubility of  
679 the ketones indicated a high loss rate. However, the signal was too noisy to determine loss rates from the data.

680 C<sub>5</sub>-aldehydes, which were usually detected together with the C<sub>5</sub>-ketones, exhibited lower mixing ratios, especially in  
681 the dry season. Overall, the mixing ratios were below their LOD and thus not investigated in detail. However, a diurnal  
682 and vertical pattern of C<sub>5</sub>-aldehydes with vertical and diurnal variabilities different to those of the C<sub>5</sub>-ketones was still  
683 apparent.

684

#### 685 **4.7 n-Hexanal/Hexenols and Hexenals**

686 C<sub>6</sub>-aldehydes, namely n-hexanal, Z-2-hexenal, Z-3-hexenal, E-2-hexenal, and E-3-hexenal, together with C<sub>6</sub>-alcohols  
687 and esters form a group that is often termed green leaf volatiles (GLV). Although different temporal variabilities were  
688 observed for n-hexanal/hexenols and hexenals, we here discuss them together in one section due to their common  
689 sources.

690 In the chloroplasts of almost all green plants, GLV are synthesized from fatty acids as part of the oxylipin pathway.  
691 Their emission results from wounding or mechanical damage, from abiotic factors (such as wind), herbivores, and  
692 pathogen attack (Scala et al., 2013). The amount of GLV emitted from corn plants has been shown to depend on soil  
693 water content, temperature, light, and fertilization, with a stronger emission response at higher temperatures  
694 (Gouinguéné and Turlings, 2002). Furthermore, emission has been reported as a response to abiotic stress from light-  
695 dark transitions (Jardine et al., 2012a). Their production and release can be very fast; in the case of Z-3-hexenal,  
696 emission begins only 1 or 2 seconds after damage (Fall et al., 1999). On one hand, GLV have antibiotic properties and  
697 protect the wounded tissue from invading bacteria or other microorganisms. On the other hand, their rapid production  
698 and release make them useful for intra and inter-chemical communication in plants, for example for priming defense  
699 mechanisms. It has been found that a herbivore-infested plant releases signaling compounds, like GLV to attract the  
700 predator (insects, beetles, birds, etc.) of the herbivore (Scala et al., 2013; Mumm and Dicke, 2010; Zannoni et al.,  
701 2020a). The release of GLV can happen on short timescales of minutes to hours but in cases of repetitive wounding



702 or drying of leaves, the emission can be continuous over days (Scala et al., 2013; Fall et al., 1999). Release of GLV is  
703 also caused by drought stress, and GLV levels have been observed to increase at noon as a result of high temperatures  
704 in the Amazon forest (Jardine et al., 2015; Kesselmeier and Staudt, 1999).

705 It remains unclear if the leaf alcohol Z-3-hexanol contributed to the hexanal signal. Z-3-hexanol is also a GLV and  
706 has been reported to represent a major part of the emission of many studied plants (Kesselmeier and Staudt, 1999). Its  
707 atmospheric lifetime was calculated to be 5 hours with respect to OH. Further, the less abundant isomers, such as Z-  
708 4-hexenol or E-2-hexenol, are also likely to contribute to the hexanal signal. Due to photolysis and reaction with OH,  
709 the lifetime of n-hexanal is about 4 hours (12 hours for oxidation by OH only), which is also true for E-2-hexenal  
710 (Jiménez et al., 2007). Z-3-hexenal has a shorter atmospheric lifetime of 3 hours (Xing et al., 2012).

711 At ATTO, the integrated emissions from a large uniform area were measured, which made it impossible to detect  
712 single wounding events, except for large-scale storm damage or human activities such as forest clearing. Measured  
713 mixing ratios were 15, 11, and 9 ppt for n-hexanal in the transition season and 26, 19, and 16 ppt in the dry season.  
714 Hexenals were detected at mixing ratios below LOD (6 ppt) for most parts of the day in the transition season, and 8  
715 ppt were measured at 80 m in the dry season. Nighttime mixing ratios of hexenals at 150 and 325 m were, however,  
716 also below the LOD (6 ppt). During both measurement phases, n-hexanal was continuously present, exhibiting a  
717 distinct diurnal cycle with maximum mixing ratios in the afternoon and higher values in the dry season. Since the  
718 emission rate of damaged leaves of hexenals was found to be higher compared to n-hexanal (Fall et al., 1999), the  
719 contribution of hexanols to the signal of n-hexanal was very likely. Average daytime mixing ratios between 40 and  
720 70 ppt have also been observed for hexanal and/or hexenols in an elevated position above the rainforest of Malaysia  
721 (Langford et al., 2010). To investigate whether the diurnal cycle results from temperature-dependent emission of GLV  
722 or additional secondary formation, measurements inside the canopy are required.

723 It was not surprising that a continuous decrease in both n-hexanal and hexenols with height was observed throughout  
724 the day, similar to propanal and other reactive primary emissions like isoprene and monoterpenes. Correlations at  
725 80 m with isoprene ( $0.78 < p < 0.86$ ), monoterpenes ( $0.74 < p < 0.91$ ), and propanal ( $p = 0.88$ , dry season) indicated  
726 light- or temperature-driven emission or rapid secondary formation close to the canopy. This correlation is interesting  
727 since GLV emissions upon biotic-induced stresses such as herbivory do not necessarily follow a diel cycle. However,  
728 boundary layer dynamics might have modulated the diel cycle since mixing between the canopy and atmosphere is  
729 most efficient during daytime convective conditions. Additionally, temperature-related drying of leaves could have  
730 led to the observed diel variability.

731 In contrast to n-hexanal/hexenols, hexenals exhibit a more pronounced seasonal variability, with very low mixing  
732 ratios, mostly below the LOD, in the transition season. The correlation with isoprene and monoterpenes during the  
733 daytime in the dry season was rather low ( $p = 0.71$ ), with the highest correlations for acetone, MEK, benzaldehyde,  
734 and ethanol ( $p > 0.8$ ), suggesting primary and secondary sources of hexenals.

735 For all C<sub>6</sub>-aldehydes investigated in this section, decreasing concentrations during nighttime at all three heights were  
736 observed in the dry season, when C<sub>6</sub>-aldehydes mixing ratios were generally higher than in the transition season. A  
737 slightly slower decrease of 80-m mixing ratios compared to the higher levels in the dry season may indicate a continued  
738 nocturnal emission of GLV, which is plausible since production and release from mechanical wounding, stress, or  
739 herbivory is possible without light (He et al., 2021).

#### 740 **4.8 Benzaldehyde**

741 The average mixing ratios of benzaldehyde measured in this study are 12, 12, 12 ppt in the transition season and 11,  
742 10, 11 ppt (80, 150, 325 m) in the dry season. No seasonal variability or vertical gradient was observed between the  
743 measurement periods.

744 Benzaldehyde is the lightest monoaromatic aldehyde and is formed via the oxidation of other aromatic compounds. It  
745 is a major intermediate product of the oxidation of benzyl radicals via OH and, thereby, of all alkyl-substituted  
746 aromatic hydrocarbons (Sebbar et al., 2011). Biogenic aromatics, such as volatile benzenoids or larger molecules like  
747 lignols, are produced via the shikimate pathway by plants, which is an important metabolic process, but benzaldehyde  
748 can also be emitted by microorganisms (Ladino-Orjuela et al., 2016; Laothawornkitkul et al., 2009). The oxidation of



749 toluene, which has previously been observed to be emitted from forested environments and farm crops (Heiden et al.,  
750 1999), yields benzaldehyde as a product (6-%) (Atkinson and Arey, 2003). Benzaldehyde is also a benzyl alcohol  
751 oxidation product, which has been reported previously to be emitted from biogenic sources (Bernard et al., 2013).  
752 Benzaldehyde is very reactive, with a calculated atmospheric lifetime primarily determined by its photolysis rate of  
753 2.4 hours (Cabrera-Perez et al., 2016) (1.7 days with respect to OH).

754 Primary emission of benzaldehyde from vegetation has been reported for grass (Kirstine et al., 1998) and elevated  
755 concentrations under and within the canopy of the Amazon rainforest were measured (Kesselmeier et al., 2000). The  
756 high mixing ratios (about 300 ppt) found at the ground were suspected to result from the decomposition of biomass,  
757 specifically the decomposition of lignols within the litter. In that study, the mixing ratios above the canopy were much  
758 lower than those measured at ground level.

759 The apparent light or temperature-driven diurnal cycle of benzaldehyde suggests secondary photochemical production  
760 from aromatic hydrocarbons, as the shikimate pathway is independent of light (Jan et al., 2021). The atmospheric  
761 lifetime of precursor aromatics ranges from days to weeks (Altshuler, 1991). Secondary production from long-lived  
762 precursors is a feasible explanation for the missing vertical variability of the very reactive benzaldehyde in the first  
763 325 m of the mixed layer. The rather slow secondary production throughout the mixed layer possibly compensated  
764 for the expected loss through oxidation and dilutive mixing. Mixing ratios observed at 80 m were only slightly more  
765 abundant in the dry season compared to higher altitudes, which could mean a stronger contribution of benzaldehyde  
766 emissions. However, the narrow vertical benzaldehyde distribution points towards well-mixed aromatic precursor  
767 hydrocarbons. Daytime mixing ratios of carbonyls that are suspected to be formed predominantly due to  
768 photochemical formation, namely, acetic acid,  $C_5H_4O_3$ , methacrolein, MVK, but also acetaldehyde and acetone,  
769 correlate very well with benzaldehyde in the dry season ( $0.85 > p > 0.95$ ). In the transition season, the correlation with  
770 the same compounds is smaller ( $0.75 > p > 0.86$ ). Possible explanations for this difference most likely lie in altered  
771 sources of precursors or benzaldehyde itself due to differences in, e.g., litter decomposing activities. It is important to  
772 note that the missing vertical variability could also be a sign of contamination from the measurement tower itself, e.g.,  
773 through temperature-dependent outgassing of its coating. However, the measurement of the fresh paint did not show  
774 elevated benzaldehyde, while the fresh anticorrosion agent emits some benzaldehyde, but at much lower rates than  
775 other VOC, e.g., toluene or xylene.

776 Globally, dry deposition constitutes a small sink of benzaldehyde in the same range as oxidation by  $NO_3$  (Cabrera-  
777 Perez et al., 2016). We observed decreasing mixing ratios at all three heights throughout the night (Table 2). Wet  
778 deposition and uptake to leaves and soil might have been the dominant sink.

779 There is evidence that benzaldehyde PAN can emerge when transported to high  $NO_x$  regions (Caralp et al., 1999).  
780 Mixing ratios of PAN are quite high so this must be considered, but photochemical PAN creation potential is the  
781 lowest of the whole group of organic compounds (Derwent et al., 1998).

782

## 783 5 Conclusion

784 In this study, a PTR-ToF-MS was operated using  $NO^+$  as the reagent ion for measuring specific carbonyl compounds  
785 at three heights (80, 150, 325 m), in two seasons, and over 24-hour cycles, on the ATTO tower located in the Brazilian  
786 Amazon rainforest. With the more commonly used ionization method for PTR-MS involving  $H_3O^+$  ions, aldehyde and  
787 ketone isomers were detected together at the same exact mass. This precludes the investigation of the individual  
788 species. For the first time, mixing ratios of biogenic aldehydes and ketones measured at high frequency are reported  
789 for a rainforest ecosystem. Generally, higher mixing ratios were found in the dry season. To some extent, this can be  
790 attributed to higher temperatures and enhanced light conditions, which drive emissions and photochemical activity.  
791 However, since temperature and PAR were only slightly enhanced in the dry season compared to the wet-to-dry  
792 transition, other aspects such as phenology (gross ecosystem productivity peaking in the dry season) and contribution  
793 of long-lived species from aged biomass burning plumes are of importance. Ketones have atmospheric lifetimes (days  
794 to weeks) that are much longer than the vertical mixing times (15–60 min) (Ringsdorf et al., 2023). Such compounds



795 can, therefore, be expected to be also present above the lowermost mixing layer (ABL) in the residual layer and free  
796 troposphere. Interestingly, elevated ketone mixing ratios in the roughness sublayer observed at 80 m by day suggest a  
797 large source at canopy level or just above. At night, the loss of these species indicates a rapid deposition to the canopy  
798 or the underlying forest floor. The correlations shown in Figures 3–4 reveal seasonal differences in the partitioning of  
799 primary emission from the canopy and the rate of rapid secondary production above the canopy. The most abundant  
800 individually measured carbonyls in this study were acetaldehyde and acetone, both effective PAN precursors, followed  
801 by isoprene oxidation products and propanal. Note that formaldehyde was not detected by the applied method. The  
802 shorter-lived, longer-chain aldehydes observed in this study showed great variation, exhibiting both increasing and  
803 decreasing vertical gradients that vary considerably in strength. All carbonyl compounds showed a distinct diurnal  
804 cycle which followed the evolution of light and temperature during the day and, for most compounds, a decrease  
805 during the night driven in part by reaction with  $\text{NO}_3$  but more importantly by deposition to plant tissues, as has been  
806 shown by flux measurements for a few oxygenated species before (Karl et al., 2004). The nocturnal uptake of these  
807 carbonyl compounds is an important aspect of their local-to-regional-scale budget. Based on this data, we hypothesize  
808 that the ecosystem can more efficiently produce reduced species such as isoprene and monoterpenes but more  
809 efficiently utilize the oxygenated products of these precursors. The importance of uptake followed by metabolism  
810 or storage, especially for oxygenated BVOC has been stressed already in the context of bidirectional exchange of  
811 BVOC by Niinemets et al. (2014). This would imply that the rainforest exploits atmospheric oxidation to convert  
812 products into more useful, metabolizable forms. Similar preferences for the uptake of oxygenated species over terpenes  
813 have been reported for epiphytes such as lichen and moss (Edtbauer et al., 2021). This idea can serve as the basic  
814 hypothesis for future plant experiments and the observed loss rates of carbonyl species can help to constrain turbulence  
815 resolving canopy exchange models. Overall, we need to improve our understanding of the complexity of biological  
816 production and consumption and invest into investigations of primary emissions on a leaf or branch level.

817 Butanal, and carbonyls higher than  $\text{C}_7$  were found to be minor components of the rainforest atmosphere, as were the  
818 alkanes isopentane, methylcyclopentane, sum of 2- and 3-methylpentane and  $\text{C}_7$  cyclic alkanes. The ratio of the  
819 aldehydes propanal and acetaldehyde, which have comparable atmospheric lifetimes and which were shown to  
820 correlate very well in previous studies, was found to be much higher with 1:4.2 and 1:7.2 in the transition and dry  
821 season at 80 m compared to the global average ratio of 1:3 (Singh et al., 2004), due to the overwhelming predominance  
822 of biogenic sources and precursors in the rainforest.

823 This application of the  $\text{NO}^+$  CIMS method has enabled the study of the individual carbonyls not accessible using the  
824  $\text{H}_3\text{O}^+$ -based method. We, therefore, recommend periodic switching of the reagents to allow for more specific detection  
825 of biogenic emissions. This would complement long-term measurements conducted using the  $\text{H}_3\text{O}^+$  ionization method.

826

827 **Code availability.** The python code can be provided upon request.

828 **Data availability.** BVOC data are available on the ATTO data portal (<https://www.attodata.org/>), a DOI is  
829 requested and will follow soon. Meteorological data conducted at the ATTO tower (320 m) in 2019 are available via  
830 <https://doi.org/10.17871/atto.95.12.742>.

831 **Supplement link:** A link to the supplement will be included by Copernicus, if applicable.

832 **Author contributions:** AR and AE conducted the BVOC measurements and AR analyzed this data and drafted the  
833 manuscript. BH and CP provided the black carbon observations and meteorological parameters conducted at the  
834 325-m-tall tower. MOS and AA conducted the measurements of the meteorological parameters at the 80 m tower.  
835 J.W. supervised this study. J.L. supervised the research that led to this study.

836 **Competing interests:** The authors declare that they have no conflict of interest.

837 **Acknowledgements:** We acknowledge the support by the German Federal Ministry of Education and Research  
838 (BMBF contract 01LB1001A and 01LK1602B) and the Brazilian Ministério da Ciência, Tecnologia e Inovação





839 (MCTI/FINEP contract 01.11.01248.00) as well as the Amazon State University (UEA), FAPESP, CNPq, FAPEAM,  
840 LBA/INPA, and SDS/CEUC/RDS-Uatumã. We thank Thomas Klüpfel for his help with VOC measurements. We  
841 especially acknowledge the technical and logistical support of the ATTO team (in particular Reiner Ditz and Hermes  
842 Braga Xavier). We also thank Andrew Crozier for creating and providing a detailed map of the ATTO site.

## 843 6 References

844 Altshuller, A. P.: Chemical reactions and transport of alkanes and their products in the troposphere, *J. Atmospheric*  
845 *Chem.*, 12, 19–61, <https://doi.org/10.1007/BF00053933>, 1991.

846 Andreae, M. O.: Emission of trace gases and aerosols from biomass burning – an updated assessment, *Atmospheric*  
847 *Chem. Phys.*, 19, 8523–8546, <https://doi.org/10.5194/acp-19-8523-2019>, 2019.

848 Andreae, M. O. and Merlet, P.: Emission of trace gases and aerosols from biomass burning, *Glob. Biogeochem.*  
849 *Cycles*, 15, 955–966, <https://doi.org/10.1029/2000GB001382>, 2001.

850 Andreae, M. O., Artaxo, P., Brandão, C., Carswell, F. E., Ciccioli, P., da Costa, A. L., Culf, A. D., Esteves, J. L.,  
851 Gash, J. H. C., Grace, J., Kabat, P., Lelieveld, J., Malhi, Y., Manzi, A. O., Meixner, F. X., Nobre, A. D., Nobre, C.,  
852 Ruivo, M. d. L. P., Silva-Dias, M. A., Stefani, P., Valentini, R., von Jouanne, J., and Waterloo, M. J.: Biogeochemical  
853 cycling of carbon, water, energy, trace gases, and aerosols in Amazonia: The LBA-EUSTACH experiments, *J.*  
854 *Geophys. Res. Atmospheres*, 107, LBA 33-1-LBA 33-25, <https://doi.org/10.1029/2001JD000524>, 2002.

855 Andreae, M. O., Acevedo, O. C., Araújo, A., Artaxo, P., Barbosa, C. G. G., Barbosa, H. M. J., Brito, J., Carbone, S.,  
856 Chi, X., Cintra, B. B. L., da Silva, N. F., Dias, N. L., Dias-Júnior, C. Q., Ditas, F., Ditz, R., Godoi, A. F. L., Godoi,  
857 R. H. M., Heimann, M., Hoffmann, T., Kesselmeier, J., Könemann, T., Krüger, M. L., Lavric, J. V., Manzi, A. O.,  
858 Lopes, A. P., Martins, D. L., Mikhailov, E. F., Moran-Zuloaga, D., Nelson, B. W., Nölscher, A. C., Santos Nogueira,  
859 D., Piedade, M. T. F., Pöhlker, C., Pöschl, U., Quesada, C. A., Rizzo, L. V., Ro, C.-U., Ruckteschler, N., Sá, L. D. A.,  
860 de Oliveira Sá, M., Sales, C. B., dos Santos, R. M. N., Saturno, J., Schöngart, J., Sörgel, M., de Souza, C. M., de  
861 Souza, R. A. F., Su, H., Targhetta, N., Tóta, J., Trebs, I., Trumbore, S., van Eijck, A., Walter, D., Wang, Z., Weber,  
862 B., Williams, J., Winderlich, J., Wittmann, F., Wolff, S., and Yáñez-Serrano, A. M.: The Amazon Tall Tower  
863 Observatory (ATTO): overview of pilot measurements on ecosystem ecology, meteorology, trace gases, and aerosols,  
864 *Atmospheric Chem. Phys.*, 15, 10723–10776, <https://doi.org/10.5194/acp-15-10723-2015>, 2015.

865 Atkinson, R. and Arey, J.: Atmospheric Degradation of Volatile Organic Compounds, *Chem. Rev.*, 103, 4605–4638,  
866 <https://doi.org/10.1021/cr0206420>, 2003.

867 Atkinson, R., Tuazon, E. C., and Aschmann, S. M.: Atmospheric Chemistry of 2-Pentanone and 2-Heptanone,  
868 *Environ. Sci. Technol.*, 34, 623–631, <https://doi.org/10.1021/es9909374>, 2000.

869 Bernard, F., Magneron, I., Eyglunent, G., Daële, V., Wallington, T. J., Hurley, M. D., and Mellouki, A.: Atmospheric  
870 Chemistry of Benzyl Alcohol: Kinetics and Mechanism of Reaction with OH Radicals, *Environ. Sci. Technol.*, 47,  
871 3182–3189, <https://doi.org/10.1021/es304600z>, 2013.

872 Bond, D. W., Steiger, S., Zhang, R., Tie, X., and Orville, R. E.: The importance of NO<sub>x</sub> production by lightning in  
873 the tropics, *Atmos. Environ.*, 36, 1509–1519, [https://doi.org/10.1016/S1352-2310\(01\)00553-2](https://doi.org/10.1016/S1352-2310(01)00553-2), 2002.

874 Boursoukidis, E., Behrendt, T., Yáñez-Serrano, A. M., Hellén, H., Diamantopoulos, E., Catão, E., Ashworth, K.,  
875 Pozzer, A., Quesada, C. A., Martins, D. L., Sá, M., Araújo, A., Brito, J., Artaxo, P., Kesselmeier, J., Lelieveld, J., and  
876 Williams, J.: Strong sesquiterpene emissions from Amazonian soils, *Nat. Commun.*, 9, 2226,  
877 <https://doi.org/10.1038/s41467-018-04658-y>, 2018.

878 Bracho-Nunez, A., Knothe, N. M., Costa, W. R., Maria Astrid, L. R., Kleiss, B., Rottenberger, S., Piedade, M. T. F.,  
879 and Kesselmeier, J.: Root anoxia effects on physiology and emissions of volatile organic compounds (VOC) under  
880 short-and long-term inundation of trees from Amazonian floodplains, *SpringerPlus*, 1, 9, <https://doi.org/10.1186/2193->  
881 1801-1-9, 2012.



- 882 Breuninger, C., Meixner, F. X., and Kesselmeier, J.: Field investigations of nitrogen dioxide (NO<sub>2</sub>) exchange between  
883 plants and the atmosphere, *Atmospheric Chem. Phys.*, 13, 773–790, <https://doi.org/10.5194/acp-13-773-2013>, 2013.
- 884 Brown, S. S. and Stutz, J.: Nighttime radical observations and chemistry, *Chem. Soc. Rev.*, 41, 6405,  
885 <https://doi.org/10.1039/c2cs35181a>, 2012.
- 886 Cabrera-Perez, D., Taraborrelli, D., Sander, R., and Pozzer, A.: Global atmospheric budget of simple monocyclic  
887 aromatic compounds, *Atmospheric Chem. Phys.*, 16, 6931–6947, <https://doi.org/10.5194/acp-16-6931-2016>, 2016.
- 888 Calogirou, A., Larsen, B. R., and Kotzias, D.: Gas-phase terpene oxidation products: a review, *Atmos. Environ.*, 33,  
889 1423–1439, [https://doi.org/10.1016/S1352-2310\(98\)00277-5](https://doi.org/10.1016/S1352-2310(98)00277-5), 1999.
- 890 Canaval, E., Millet, D. B., Zimmer, I., Nosenko, T., Georgii, E., Partoll, E. M., Fischer, L., Alwe, H. D., Kulmala, M.,  
891 Karl, T., Schnitzler, J.-P., and Hansel, A.: Rapid conversion of isoprene photooxidation products in terrestrial plants,  
892 *Commun. Earth Environ.*, 1, 1–9, <https://doi.org/10.1038/s43247-020-00041-2>, 2020.
- 893 Cappellin, L., Karl, T., Probst, M., Ismailova, O., Winkler, P. M., Soukoulis, C., Aprea, E., Märk, T. D., Gasperi, F.,  
894 and Biasioli, F.: On Quantitative Determination of Volatile Organic Compound Concentrations Using Proton Transfer  
895 Reaction Time-of-Flight Mass Spectrometry, *Environ. Sci. Technol.*, 46, 2283–2290,  
896 <https://doi.org/10.1021/es203985t>, 2012.
- 897 Caralp, F., Foucher, V., Lesclaux, R., Wallington, T. J., and Hurley, M. D.: Atmospheric chemistry of benzaldehyde:  
898 UV absorption spectrum and reaction kinetics and mechanisms of the C<sub>6</sub>H<sub>5</sub>C(O)O<sub>2</sub> radical, *Phys. Chem. Chem.  
899 Phys.*, 1, 3509–3517, <https://doi.org/10.1039/a903088c>, 1999.
- 900 Chamecki, M., Freire, L. S., Dias, N. L., Chen, B., Dias-Junior, C. Q., Machado, L. A. T., Sörgel, M., Tsokankunku,  
901 A., and Araújo, A. C. de: Effects of Vegetation and Topography on the Boundary Layer Structure above the Amazon  
902 Forest, *J. Atmospheric Sci.*, 77, 2941–2957, <https://doi.org/10.1175/JAS-D-20-0063.1>, 2020.
- 903 Chaparro-Suarez, I. G., Meixner, F. X., and Kesselmeier, J.: Nitrogen dioxide (NO<sub>2</sub>) uptake by vegetation controlled  
904 by atmospheric concentrations and plant stomatal aperture, *Atmos. Environ.*, 45, 5742–5750,  
905 <https://doi.org/10.1016/j.atmosenv.2011.07.021>, 2011.
- 906 Chen, Y., Yuan, B., Wang, C., Wang, S., He, X., Wu, C., Song, X., Huangfu, Y., Li, X.-B., Liao, Y., and Shao, M.:  
907 Online measurements of cycloalkanes based on NO<sup>+</sup> chemical ionization in proton transfer reaction time-of-flight  
908 mass spectrometry (PTR-ToF-MS), *Atmospheric Meas. Tech.*, 15, 6935–6947, <https://doi.org/10.5194/amt-15-6935-2022>, 2022.
- 910 Chevaturi, A., Klingaman, N. P., Rudorff, C. M., Coelho, C. A. S., and Schöngart, J.: Forecasting annual maximum  
911 water level for the Negro River at Manaus, *Clim. Resil. Sustain.*, 1, e18, <https://doi.org/10.1002/cli2.18>, 2022.
- 912 Ciccioi, P., Silibello, C., Finardi, S., Pepe, N., Ciccioi, P., Rapparini, F., Neri, L., Fares, S., Brilli, F., Mircea, M.,  
913 Magliulo, E., and Baraldi, R.: The potential impact of biogenic volatile organic compounds (BVOCs) from terrestrial  
914 vegetation on a Mediterranean area using two different emission models, *Agric. For. Meteorol.*, 328, 109255,  
915 <https://doi.org/10.1016/j.agrformet.2022.109255>, 2023.
- 916 Colomb, A., Williams, J., Crowley, J., Gros, V., Hofmann, R., Salisbury, G., Klüpfel, T., Kormann, R., Stickler, A.,  
917 Forster, C., and Lelieveld, J.: Airborne Measurements of Trace Organic Species in the Upper Troposphere Over  
918 Europe: the Impact of Deep Convection, *Environ. Chem.*, 3, 244–259, <https://doi.org/10.1071/EN06020>, 2006.
- 919 Deming, B. L., Pagonis, D., Liu, X., Day, D. A., Talukdar, R., Krechmer, J. E., de Gouw, J. A., Jimenez, J. L., and  
920 Ziemann, P. J.: Measurements of delays of gas-phase compounds in a wide variety of tubing materials due to gas–  
921 wall interactions, *Atmospheric Meas. Tech.*, 12, 3453–3461, <https://doi.org/10.5194/amt-12-3453-2019>, 2019.





- 922 Derwent, R. G., Jenkin, M. E., Saunders, S. M., and Pilling, M. J.: Photochemical ozone creation potentials for organic  
923 compounds in northwest Europe calculated with a master chemical mechanism, *Atmos. Environ.*, 32, 2429–2441,  
924 [https://doi.org/10.1016/S1352-2310\(98\)00053-3](https://doi.org/10.1016/S1352-2310(98)00053-3), 1998.
- 925 Edtbauer, A., Pfannerstill, E. Y., Pires Florentino, A. P., Barbosa, C. G. G., Rodriguez-Caballero, E., Zannoni, N.,  
926 Alves, R. P., Wolff, S., Tsokankunku, A., Aptroot, A., de Oliveira Sá, M., de Araújo, A. C., Sörgel, M., de Oliveira,  
927 S. M., Weber, B., and Williams, J.: Cryptogamic organisms are a substantial source and sink for volatile organic  
928 compounds in the Amazon region, *Commun. Earth Environ.*, 2, 1–14, <https://doi.org/10.1038/s43247-021-00328-y>,  
929 2021.
- 930 Ernle, L., Wang, N., Bekö, G., Morrison, G., Wargocki, P., J. Weschler, C., and Williams, J.: Assessment of aldehyde  
931 contributions to PTR-MS  $m/z$  69.07 in indoor air measurements, *Environ. Sci. Atmospheres*, 3, 1286–1295,  
932 <https://doi.org/10.1039/D3EA00055A>, 2023.
- 933 Fall, R.: Abundant Oxygenates in the Atmosphere: A Biochemical Perspective, *Chem. Rev.*, 103, 4941–4952,  
934 <https://doi.org/10.1021/cr0206521>, 2003.
- 935 Fall, R., Karl, T., Hansel, A., Jordan, A., and Lindinger, W.: Volatile organic compounds emitted after leaf wounding:  
936 On-line analysis by proton-transfer-reaction mass spectrometry, *J. Geophys. Res. Atmospheres*, 104, 15963–15974,  
937 <https://doi.org/10.1029/1999JD900144>, 1999.
- 938 Fischer, E. V., Jacob, D. J., Yantosca, R. M., Sulprizio, M. P., Millet, D. B., Mao, J., Paulot, F., Singh, H. B., Roiger,  
939 A., Ries, L., Talbot, R. W., Dzepina, K., and Pandey Deolal, S.: Atmospheric peroxyacetyl nitrate (PAN): a global  
940 budget and source attribution, *Atmospheric Chem. Phys.*, 14, 2679–2698, <https://doi.org/10.5194/acp-14-2679-2014>,  
941 2014.
- 942 Fruekilde, P., Hjorth, J., Jensen, N. R., Kotzias, D., and Larsen, B.: OZONOLYSIS AT VEGETATION SURFACES:  
943 A SOURCE OF ACETONE, 4-OXOPENTANAL, 6-METHYL-5-HEPTEN-2-ONE, AND GERANYL ACETONE  
944 IN THE TROPOSPHERE, *Atmos. Environ.*, Vol. 32, No. 11, 1893–1902, 1998.
- 945 Fuentes, J. D., Gerken, T., Chamecki, M., Stoy, P., Freire, L., and Ruiz-Plancarte, J.: Turbulent transport and reactions  
946 of plant-emitted hydrocarbons in an Amazonian rain forest, *Atmos. Environ.*, 279, 119094,  
947 <https://doi.org/10.1016/j.atmosenv.2022.119094>, 2022.
- 948 Gouinguéné, S. P. and Turlings, T. C. J.: The Effects of Abiotic Factors on Induced Volatile Emissions in Corn Plants,  
949 *Plant Physiol.*, 129, 1296–1307, <https://doi.org/10.1104/pp.001941>, 2002.
- 950 de Gouw, J. and Warneke, C.: Measurements of volatile organic compounds in the earth's atmosphere using proton-  
951 transfer-reaction mass spectrometry, *Mass Spectrom. Rev.*, 26, 223–257, <https://doi.org/10.1002/mas.20119>, 2007.
- 952 Guenther, A.: Natural emissions of non-methane volatile organic compounds, carbon monoxide, and oxides of  
953 nitrogen from North America, *Atmos. Environ.*, 34, 2205–2230, [https://doi.org/10.1016/S1352-2310\(99\)00465-3](https://doi.org/10.1016/S1352-2310(99)00465-3),  
954 2000.
- 955 Guenther, A.: Biological and Chemical Diversity of Biogenic Volatile Organic Emissions into the Atmosphere, *Int.*  
956 *Sch. Res. Not.*, 2013, e786290, <https://doi.org/10.1155/2013/786290>, 2013.
- 957 Guimbaud, C., Catoire, V., Bergeat, A., Michel, E., Schoon, N., Amelynck, C., Labonnette, D., and Poulet, G.:  
958 Kinetics of the reactions of acetone and glyoxal with  $O_2^+$  and  $NO^+$  ions and application to the detection of oxygenated  
959 volatile organic compounds in the atmosphere by chemical ionization mass spectrometry, *Int. J. Mass Spectrom.*, 263,  
960 276–288, <https://doi.org/10.1016/j.ijms.2007.03.006>, 2007.
- 961 He, J., Halitschke, R., Schuman, M. C., and Baldwin, I. T.: Light dominates the diurnal emissions of herbivore-induced  
962 volatiles in wild tobacco, *BMC Plant Biol.*, 21, 401, <https://doi.org/10.1186/s12870-021-03179-z>, 2021.



- 963 Heiden, A. C., Kobel, K., Komenda, M., Koppmann, R., Shao, M., and Wildt, J.: Toluene emissions from plants,  
964 *Geophys. Res. Lett.*, 26, 1283–1286, <https://doi.org/10.1029/1999GL900220>, 1999.
- 965 Hellén, H., Hakola, H., Reissell, A., and Ruuskanen, T. M.: Carbonyl compounds in boreal coniferous forest air in  
966 Hyytiälä, Southern Finland, *Atmospheric Chem. Phys.*, 4, 1771–1780, <https://doi.org/10.5194/acp-4-1771-2004>,  
967 2004.
- 968 Holanda, B. A., Pöhlker, M. L., Walter, D., Saturno, J., Sörgel, M., Ditas, J., Ditas, F., Schulz, C., Franco, M. A.,  
969 Wang, Q., Donth, T., Artaxo, P., Barbosa, H. M. J., Borrmann, S., Braga, R., Brito, J., Cheng, Y., Dollner, M., Kaiser,  
970 J. W., Klimach, T., Knote, C., Krüger, O. O., Fütterer, D., Lavrič, J. V., Ma, N., Machado, L. A. T., Ming, J., Morais,  
971 F. G., Paulsen, H., Sauer, D., Schlager, H., Schneider, J., Su, H., Weinzierl, B., Walser, A., Wendisch, M., Ziereis, H.,  
972 Zöger, M., Pöschl, U., Andreae, M. O., and Pöhlker, C.: Influx of African biomass burning aerosol during the  
973 Amazonian dry season through layered transatlantic transport of black carbon-rich smoke, *Atmospheric Chem. Phys.*,  
974 20, 4757–4785, <https://doi.org/10.5194/acp-20-4757-2020>, 2020.
- 975 Holanda, B. A., Franco, M. A., Walter, D., Artaxo, P., Carbone, S., Cheng, Y., Chowdhury, S., Ditas, F., Gysel-Beer,  
976 M., Klimach, T., Kremper, L. A., Krüger, O. O., Lavric, J. V., Lelieveld, J., Ma, C., Machado, L. A. T., Modini, R.  
977 L., Morais, F. G., Pozzer, A., Saturno, J., Su, H., Wendisch, M., Wolff, S., Pöhlker, M. L., Andreae, M. O., Pöschl,  
978 U., and Pöhlker, C.: African biomass burning affects aerosol cycling over the Amazon, *Commun. Earth Environ.*, 4,  
979 1–15, <https://doi.org/10.1038/s43247-023-00795-5>, 2023.
- 980 Holzinger, R., Sandoval-Soto, L., Rottenberger, S., Crutzen, P. J., and Kesselmeier, J.: Emissions of volatile organic  
981 compounds from *Quercus ilex* L. measured by Proton Transfer Reaction Mass Spectrometry under different  
982 environmental conditions, *J. Geophys. Res. Atmospheres*, 105, 20573–20579, <https://doi.org/10.1029/2000JD900296>,  
983 2000.
- 984 Holzinger, R., Lee, A., Paw, K. T., and Goldstein, U. a. H.: Observations of oxidation products above a forest imply  
985 biogenic emissions of very reactive compounds, *Atmospheric Chem. Phys.*, 5, 67–75, [https://doi.org/10.5194/acp-5-](https://doi.org/10.5194/acp-5-67-2005)  
986 67-2005, 2005.
- 987 Hunter, E. P. L. and Lias, S. G.: Evaluated Gas Phase Basicities and Proton Affinities of Molecules: An Update, *J.*  
988 *Phys. Chem. Ref. Data*, 27, 413–656, <https://doi.org/10.1063/1.556018>, 1998.
- 989 Isidorov, V. A., Zenkevich, I. G., and Ioffe, B. V.: Volatile organic compounds in the atmosphere of forests,  
990 *Atmospheric Environ.* 1967, 19, 1–8, [https://doi.org/10.1016/0004-6981\(85\)90131-3](https://doi.org/10.1016/0004-6981(85)90131-3), 1985.
- 991 Jacob, D. J., Field, B. D., Jin, E. M., Bey, I., Li, Q., Logan, J. A., Yantosca, R. M., and Singh, H. B.: Atmospheric  
992 budget of acetone, *J. Geophys. Res. Atmospheres*, 107, ACH 5-1-ACH 5-17, <https://doi.org/10.1029/2001JD000694>,  
993 2002.
- 994 Jan, R., Asaf, S., Numan, M., Lubna, and Kim, K.-M.: Plant Secondary Metabolite Biosynthesis and Transcriptional  
995 Regulation in Response to Biotic and Abiotic Stress Conditions, *Agronomy*, 11, 968,  
996 <https://doi.org/10.3390/agronomy11050968>, 2021.
- 997 Jardine, K., Barron-Gafford, G. A., Norman, J. P., Abrell, L., Monson, R. K., Meyers, K. T., Pavao-Zuckerman, M.,  
998 Dontsova, K., Kleist, E., Werner, C., and Huxman, T. E.: Green leaf volatiles and oxygenated metabolite emission  
999 bursts from mesquite branches following light–dark transitions, *Photosynth. Res.*, 113, 321–333,  
1000 <https://doi.org/10.1007/s11120-012-9746-5>, 2012a.
- 1001 Jardine, K. J., Monson, R. K., Abrell, L., Saleska, S. R., Arneth, A., Jardine, A., Ishida, F. Y., Serrano, A. M. Y.,  
1002 Artaxo, P., Karl, T., Fares, S., Goldstein, A., Loreto, F., and Huxman, T.: Within-plant isoprene oxidation confirmed  
1003 by direct emissions of oxidation products methyl vinyl ketone and methacrolein, *Glob. Change Biol.*, 18, 973–984,  
1004 <https://doi.org/10.1111/j.1365-2486.2011.02610.x>, 2012b.



- 1005 Jardine, K. J., Meyers, K., Abrell, L., Alves, E. G., Yanez Serrano, A. M., Kesselmeier, J., Karl, T., Guenther, A.,  
1006 Vickers, C., and Chambers, J. Q.: Emissions of putative isoprene oxidation products from mango branches under  
1007 abiotic stress, *J. Exp. Bot.*, 64, 3669–3679, <https://doi.org/10.1093/jxb/ert202>, 2013.
- 1008 Jardine, K. J., Chambers, J. Q., Holm, J., Jardine, A. B., Fontes, C. G., Zorzanelli, R. F., Meyers, K. T., De Souza, V.  
1009 F., Garcia, S., Gimenez, B. O., Piva, L. R. de O., Higuchi, N., Artaxo, P., Martin, S., and Manzi, A. O.: Green Leaf  
1010 Volatile Emissions during High Temperature and Drought Stress in a Central Amazon Rainforest, *Plants*, 4, 678–690,  
1011 <https://doi.org/10.3390/plants4030678>, 2015.
- 1012 Jiménez, E., Lanza, B., Martínez, E., and Albaladejo, J.: Daytime tropospheric loss of hexanal and *trans*-2-  
1013 hexenal: OH kinetics and UV photolysis, *Atmospheric Chem. Phys.*, 7, 1565–1574, [https://doi.org/10.5194/acp-7-](https://doi.org/10.5194/acp-7-1565-2007)  
1014 1565-2007, 2007.
- 1015 Jordan, A., Haidacher, S., Hanel, G., Hartungen, E., Märk, L., Seehauser, H., Schotzkowsky, R., Sulzer, P., and Märk,  
1016 T. D.: A high resolution and high sensitivity proton-transfer-reaction time-of-flight mass spectrometer (PTR-TOF-  
1017 MS), *Int. J. Mass Spectrom.*, 286, 122–128, <https://doi.org/10.1016/j.ijms.2009.07.005>, 2009.
- 1018 Jordi Vilà-Guerau de Arellano, C. C. van H., Bart J. H. van Stratum, and Kees van den Dries: *Atmospheric Boundary*  
1019 *Layer*, Cambridge University Press, 2015.
- 1020 Kalalian, C., Abis, L., Depoorter, A., Lunardelli, B., Perrier, S., and George, C.: Influence of indoor chemistry on the  
1021 emission of mVOCs from *Aspergillus niger* molds, *Sci. Total Environ.*, 741, 140148,  
1022 <https://doi.org/10.1016/j.scitotenv.2020.140148>, 2020.
- 1023 Karl, T., Guenther, A., Spirig, C., Hansel, A., and Fall, R.: Seasonal variation of biogenic VOC emissions above a  
1024 mixed hardwood forest in northern Michigan, *Geophys. Res. Lett.*, 30, <https://doi.org/10.1029/2003GL018432>, 2003.
- 1025 Karl, T., Potosnak, M., Guenther, A., Clark, D., Walker, J., Herrick, J. D., and Geron, C.: Exchange processes of  
1026 volatile organic compounds above a tropical rain forest: Implications for modeling tropospheric chemistry above dense  
1027 vegetation, *J. Geophys. Res. Atmospheres*, 109, <https://doi.org/10.1029/2004JD004738>, 2004.
- 1028 Karl, T., Hansel, A., Cappellin, L., Kaser, L., Herdinger-Blatt, I., and Jud, W.: Selective measurements of isoprene  
1029 and 2-methyl-3-buten-2-ol based on NO<sup>+</sup> and ionization mass spectrometry, *Atmospheric Chem.*  
1030 *Phys.*, 12, 11877–11884, <https://doi.org/10.5194/acp-12-11877-2012>, 2012.
- 1031 Kesselmeier, J.: Exchange of Short-Chain Oxygenated Volatile Organic Compounds (VOCs) between Plants and the  
1032 Atmosphere: A Compilation of Field and Laboratory Studies, *J. Atmospheric Chem.*, 39, 219–233,  
1033 <https://doi.org/10.1023/A:1010632302076>, 2001.
- 1034 Kesselmeier, J. and Staudt, M.: Biogenic Volatile Organic Compounds (VOC): An Overview on Emission, Physiology  
1035 and Ecology, *J. Atmospheric Chem.*, 33, 23–88, <https://doi.org/10.1023/A:1006127516791>, 1999.
- 1036 Kesselmeier, J., Bode, K., Hofmann, U., Müller, H., Schäfer, L., Wolf, A., Ciccioli, P., Brancaleoni, E., Cecinato, A.,  
1037 Frattoni, M., Foster, P., Ferrari, C., Jacob, V., Fugit, J. L., Dutaur, L., Simon, V., and Torres, L.: Emission of short  
1038 chained organic acids, aldehydes and monoterpenes from *Quercus ilex* L. and *Pinus pinea* L. in relation to  
1039 physiological activities, carbon budget and emission algorithms, *Atmos. Environ.*, 31, 119–133,  
1040 [https://doi.org/10.1016/S1352-2310\(97\)00079-4](https://doi.org/10.1016/S1352-2310(97)00079-4), 1997.
- 1041 Kesselmeier, J., Kuhn, U., Wolf, A., Andreae, M. O., Ciccioli, P., Brancaleoni, E., Frattoni, M., Guenther, A.,  
1042 Greenberg, J., De Castro Vasconcellos, P., de Oliva, T., Tavares, T., and Artaxo, P.: Atmospheric volatile organic  
1043 compounds (VOC) at a remote tropical forest site in central Amazonia, *Atmos. Environ.*, 34, 4063–4072,  
1044 [https://doi.org/10.1016/S1352-2310\(00\)00186-2](https://doi.org/10.1016/S1352-2310(00)00186-2), 2000.



- 1045 Khan, M. A. H., Cooke, M. C., Utembe, S. R., Archibald, A. T., Derwent, R. G., Xiao, P., Percival, C. J., Jenkin, M.  
1046 E., Morris, W. C., and Shallcross, D. E.: Global modeling of the nitrate radical (NO<sub>3</sub>) for present and pre-industrial  
1047 scenarios, *Atmospheric Res.*, 164–165, 347–357, <https://doi.org/10.1016/j.atmosres.2015.06.006>, 2015.
- 1048 Kirstine, W., Galbally, I., Ye, Y., and Hooper, M.: Emissions of volatile organic compounds (primarily oxygenated  
1049 species) from pasture, *J. Geophys. Res. Atmospheres*, 103, 10605–10619, <https://doi.org/10.1029/97JD03753>, 1998.
- 1050 Kirstine, W. V. and Galbally, I. E.: The global atmospheric budget of ethanol revisited, *Atmospheric Chem. Phys.*,  
1051 12, 545–555, <https://doi.org/10.5194/acp-12-545-2012>, 2012.
- 1052 König, G., Brunda, M., Puxbaum, H., Hewitt, C. N., Duckham, S. C., and Rudolph, J.: Relative contribution of  
1053 oxygenated hydrocarbons to the total biogenic VOC emissions of selected mid-European agricultural and natural plant  
1054 species, *Atmos. Environ.*, 29, 861–874, [https://doi.org/10.1016/1352-2310\(95\)00026-U](https://doi.org/10.1016/1352-2310(95)00026-U), 1995.
- 1055 Koss, A. R., Warneke, C., Yuan, B., Coggon, M. M., Veres, P. R., and de Gouw, J. A.: Evaluation of  
1056 NO<sub>3</sub> reagent ion chemistry for online measurements of atmospheric volatile organic  
1057 compounds, *Atmospheric Meas. Tech.*, 9, 2909–2925, <https://doi.org/10.5194/amt-9-2909-2016>, 2016.
- 1058 Kreuzwieser, J., Kühnemann, F., Martis, A., Rennenberg, H., and Urban, W.: Diurnal pattern of acetaldehyde emission  
1059 by flooded poplar trees, *Physiol. Plant.*, 108, 79–86, <https://doi.org/10.1034/j.1399-3054.2000.108001079.x>, 2000.
- 1060 Kuhn, U., Rottenberger, S., Biesenthal, T., Wolf, A., Schebeske, G., Ciccioli, P., Brancaleoni, E., Frattoni, M.,  
1061 Tavares, T. M., and Kesselmeier, J.: Seasonal differences in isoprene and light-dependent monoterpene emission by  
1062 Amazonian tree species, *Glob. Change Biol.*, 10, 663–682, <https://doi.org/10.1111/j.1529-8817.2003.00771.x>, 2004a.
- 1063 Kuhn, U., Rottenberger, S., Biesenthal, T., Wolf, A., Schebeske, G., Ciccioli, P., and Kesselmeier, J.: Strong  
1064 correlation between isoprene emission and gross photosynthetic capacity during leaf phenology of the tropical tree  
1065 species *Hymenaea courbaril* with fundamental changes in volatile organic compounds emission composition during  
1066 early leaf development, *Plant Cell Environ.*, 27, 1469–1485, <https://doi.org/10.1111/j.1365-3040.2004.01252.x>,  
1067 2004b.
- 1068 Kuhn, U., Andreae, M. O., Ammann, C., Araújo, A. C., Brancaleoni, E., Ciccioli, P., Dindorf, T., Frattoni, M., Gatti,  
1069 L. V., Ganzeveld, L., Kruijt, B., Lelieveld, J., Lloyd, J., Meixner, F. X., Nobre, A. D., Pöschl, U., Spirig, C., Stefani,  
1070 P., Thielmann, A., Valentini, R., and Kesselmeier, J.: Isoprene and monoterpene fluxes from Central Amazonian  
1071 rainforest inferred from tower-based and airborne measurements, and implications on the atmospheric chemistry and  
1072 the local carbon budget, *Atmospheric Chem. Phys.*, 7, 2855–2879, <https://doi.org/10.5194/acp-7-2855-2007>, 2007.
- 1073 Ladino-Orjuela, G., Gomes, E., da Silva, R., Salt, C., and Parsons, J. R.: Metabolic Pathways for Degradation of  
1074 Aromatic Hydrocarbons by Bacteria, in: *Reviews of Environmental Contamination and Toxicology Volume 237*, vol.  
1075 237, edited by: de Voogt, W. P., Springer International Publishing, Cham, 105–121, [https://doi.org/10.1007/978-3-319-23573-8\\_5](https://doi.org/10.1007/978-3-319-23573-8_5), 2016.
- 1077 Langford, B., Misztal, P. K., Nemitz, E., Davison, B., Helfter, C., Pugh, T. a. M., MacKenzie, A. R., Lim, S. F., and  
1078 Hewitt, C. N.: Fluxes and concentrations of volatile organic compounds from a South-East Asian tropical rainforest,  
1079 *Atmospheric Chem. Phys.*, 10, 8391–8412, <https://doi.org/10.5194/acp-10-8391-2010>, 2010.
- 1080 Laothawornkitkul, J., Taylor, J. E., Paul, N. D., and Hewitt, C. N.: Biogenic volatile organic compounds in the Earth  
1081 system, *New Phytol.*, 183, 27–51, <https://doi.org/10.1111/j.1469-8137.2009.02859.x>, 2009.
- 1082 Lary, D. J. and Shallcross, D. E.: Central role of carbonyl compounds in atmospheric chemistry, *J. Geophys. Res.*  
1083 *Atmospheres*, 105, 19771–19778, <https://doi.org/10.1029/1999JD901184>, 2000.
- 1084 Lelieveld, J., Gromov, S., Pozzer, A., and Taraborrelli, D.: Global tropospheric hydroxyl distribution, budget and  
1085 reactivity, *Atmospheric Chem. Phys.*, 16, 12477–12493, <https://doi.org/10.5194/acp-16-12477-2016>, 2016.



- 1086 Lewis, H. L.: Caproic Acid Metabolism and the Production of 2-Pentanone and Gluconic Acid by *Aspergillus niger*,  
1087 *Microbiology*, 63, 203–210, <https://doi.org/10.1099/00221287-63-2-203>, 1970.
- 1088 Li, X.-B., Zhang, C., Liu, A., Yuan, B., Yang, H., Liu, C., Wang, S., Huangfu, Y., Qi, J., Liu, Z., He, X., Song, X.,  
1089 Chen, Y., Peng, Y., Zhang, X., Zheng, E., Yang, L., Yang, Q., Qin, G., Zhou, J., and Shao, M.: Assessment of long  
1090 tubing in measuring atmospheric trace gases: applications on tall towers, *Environ. Sci. Atmospheres*, 3, 506–520,  
1091 <https://doi.org/10.1039/D2EA00110A>, 2023.
- 1092 Liu, Q., Gao, Y., Huang, W., Ling, Z., Wang, Z., and Wang, X.: Carbonyl compounds in the atmosphere: A review  
1093 of abundance, source and their contributions to O<sub>3</sub> and SOA formation, *Atmospheric Res.*, 274, 106184,  
1094 <https://doi.org/10.1016/j.atmosres.2022.106184>, 2022.
- 1095 Liu, Y., Brito, J., Dorris, M. R., Rivera-Rios, J. C., Seco, R., Bates, K. H., Artaxo, P., Duvoisin, S., Keutsch, F. N.,  
1096 Kim, S., Goldstein, A. H., Guenther, A. B., Manzi, A. O., Souza, R. A. F., Springston, S. R., Watson, T. B., McKinney,  
1097 K. A., and Martin, S. T.: Isoprene photochemistry over the Amazon rainforest, *Proc. Natl. Acad. Sci.*, 113, 6125–  
1098 6130, <https://doi.org/10.1073/pnas.1524136113>, 2016.
- 1099 Matsui, K., Sugimoto, K., Kakumyan, P., Khorobrykh, S. A., and Mano, J.: Volatile Oxylipins and Related  
1100 Compounds Formed Under Stress in Plants, in: *Lipidomics: Volume 2: Methods and Protocols*, edited by: Armstrong,  
1101 D., Humana Press, Totowa, NJ, 17–28, [https://doi.org/10.1007/978-1-60761-325-1\\_2](https://doi.org/10.1007/978-1-60761-325-1_2), 2010.
- 1102 Mellouki, A., Wallington, T. J., and Chen, J.: Atmospheric Chemistry of Oxygenated Volatile Organic Compounds:  
1103 Impacts on Air Quality and Climate, *Chem. Rev.*, 115, 3984–4014, <https://doi.org/10.1021/cr500549n>, 2015.
- 1104 Mumm, R. and Dicke, M.: Variation in natural plant products and the attraction of bodyguards involved in indirect  
1105 plant defense, *Can. J. Zool.*, 88, 628–667, <https://doi.org/10.1139/Z10-032>, 2010.
- 1106 Nguyen, T. B., Crounse, J. D., Teng, A. P., St. Clair, J. M., Paulot, F., Wolfe, G. M., and Wennberg, P. O.: Rapid  
1107 deposition of oxidized biogenic compounds to a temperate forest, *Proc. Natl. Acad. Sci.*, 112, E392–E401,  
1108 <https://doi.org/10.1073/pnas.1418702112>, 2015.
- 1109 Niinemets, Ü., Fares, S., Harley, P., and Jardine, K. J.: Bidirectional exchange of biogenic volatiles with vegetation:  
1110 emission sources, reactions, breakdown and deposition, *Plant Cell Environ.*, 37, 1790–1809,  
1111 <https://doi.org/10.1111/pce.12322>, 2014.
- 1112 Orzechowska, G. E., Nguyen, H. T., and Paulson, S. E.: Photochemical Sources of Organic Acids. 2. Formation of  
1113 C<sub>5</sub>–C<sub>9</sub> Carboxylic Acids from Alkene Ozonolysis under Dry and Humid Conditions, *J. Phys. Chem. A*, 109, 5366–  
1114 5375, <https://doi.org/10.1021/jp050167k>, 2005.
- 1115 Pagonis, D., Krechmer, J. E., de Gouw, J., Jimenez, J. L., and Ziemann, P. J.: Effects of gas–wall partitioning in Teflon  
1116 tubing and instrumentation on time-resolved measurements of gas-phase organic compounds, *Atmospheric Meas.*  
1117 *Tech.*, 10, 4687–4696, <https://doi.org/10.5194/amt-10-4687-2017>, 2017.
- 1118 Parolin, P., De Simone, O., Haase, K., Waldhoff, D., Rottenberger, S., Kuhn, U., Kesselmeier, J., Kleiss, B., Schmidt,  
1119 W., Pledade, M. T. F., and Junk, W. J.: Central Amazonian floodplain forests: Tree adaptations in a pulsing system,  
1120 *Bot. Rev.*, 70, 357–380, [https://doi.org/10.1663/0006-8101\(2004\)070\[0357:CAFFTA\]2.0.CO;2](https://doi.org/10.1663/0006-8101(2004)070[0357:CAFFTA]2.0.CO;2), 2004.
- 1121 Pfannerstill, E. Y., Reijrink, N. G., Edtbauer, A., Ringsdorf, A., Zannoni, N., Araújo, A., Ditas, F., Holanda, B. A.,  
1122 Sá, M. O., Tsokankunku, A., Walter, D., Wolff, S., Lavrič, J. V., Pöhlker, C., Sörgel, M., and Williams, J.: Total OH  
1123 reactivity over the Amazon rainforest: variability with temperature, wind, rain, altitude, time of day, season, and an  
1124 overall budget closure, *Atmospheric Chem. Phys.*, 21, 6231–6256, <https://doi.org/10.5194/acp-21-6231-2021>, 2021.
- 1125 Pöhlker, C., Walter, D., Paulsen, H., Könemann, T., Rodríguez-Caballero, E., Moran-Zuloaga, D., Brito, J., Carbone,  
1126 S., Degrendele, C., Després, V. R., Ditas, F., Holanda, B. A., Kaiser, J. W., Lammel, G., Lavrič, J. V., Jing, M.,  
1127 Pickersgill, D., Pöhlker, M. L., Praß, M., Löbs, N., Saturno, J., Sörgel, M., Wang, Q., Weber, B., Wolff, S., Artaxo,



- 1128 P., Pöschl, U., and Andreae, M. O.: Land cover and its transformation in the backward trajectory footprint region of  
1129 the Amazon Tall Tower Observatory, *Atmospheric Chem. Phys.*, 19, 8425–8470, [https://doi.org/10.5194/acp-19-](https://doi.org/10.5194/acp-19-8425-2019)  
1130 8425-2019, 2019.
- 1131 Prather, M. J. and Jacob, D. J.: A persistent imbalance in HO<sub>x</sub> and NO<sub>x</sub> photochemistry of the upper troposphere  
1132 driven by deep tropical convection, *Geophys. Res. Lett.*, 24, 3189–3192, <https://doi.org/10.1029/97GL03027>, 1997.
- 1133 Restrepo-Coupe, N., da Rocha, H. R., Hutyra, L. R., da Araujo, A. C., Borma, L. S., Christoffersen, B., Cabral, O. M.  
1134 R., de Camargo, P. B., Cardoso, F. L., da Costa, A. C. L., Fitzjarrald, D. R., Goulden, M. L., Kruijt, B., Maia, J. M.  
1135 F., Malhi, Y. S., Manzi, A. O., Miller, S. D., Nobre, A. D., von Randow, C., Sá, L. D. A., Sakai, R. K., Tota, J., Wofsy,  
1136 S. C., Zanchi, F. B., and Saleska, S. R.: What drives the seasonality of photosynthesis across the Amazon basin? A  
1137 cross-site analysis of eddy flux tower measurements from the Brasil flux network, *Agric. For. Meteorol.*, 182–183,  
1138 128–144, <https://doi.org/10.1016/j.agrformet.2013.04.031>, 2013.
- 1139 Ringsdorf, A., Edtbauer, A., Vilà-Guerau de Arellano, J., Pfannerstill, E. Y., Gromov, S., Kumar, V., Pozzer, A.,  
1140 Wolff, S., Tsokankunku, A., Soergel, M., Sá, M. O., Araújo, A., Ditas, F., Poehlker, C., Lelieveld, J., and Williams,  
1141 J.: Inferring the diurnal variability of OH radical concentrations over the Amazon from BVOC measurements, *Sci.*  
1142 *Rep.*, 13, 14900, <https://doi.org/10.1038/s41598-023-41748-4>, 2023.
- 1143 Rivera-Rios, J. C., Nguyen, T. B., Crounse, J. D., Jud, W., St. Clair, J. M., Mikoviny, T., Gilman, J. B., Lerner, B. M.,  
1144 Kaiser, J. B., Gouw, J., Wisthaler, A., Hansel, A., Wennberg, P. O., Seinfeld, J. H., and Keutsch, F. N.: Conversion  
1145 of hydroperoxides to carbonyls in field and laboratory instrumentation: Observational bias in diagnosing pristine  
1146 versus anthropogenically controlled atmospheric chemistry, *Geophys. Res. Lett.*, 41, 8645–8651,  
1147 <https://doi.org/10.1002/2014GL061919>, 2014.
- 1148 Roberts, J. M: PAN and Related Compounds, in: *Volatile Organic Compounds in the Atmosphere*, Blackwell  
1149 Publishing Ltd, 2007.
- 1150 Romano, A. and Hanna, G. B.: Identification and quantification of VOCs by proton transfer reaction time of flight  
1151 mass spectrometry: An experimental workflow for the optimization of specificity, sensitivity, and accuracy, *J. Mass*  
1152 *Spectrom.*, 53, 287–295, <https://doi.org/10.1002/jms.4063>, 2018.
- 1153 Rottenberger, S., Kuhn, U., Wolf, A., Schebeske, G., Oliva, S. T., Tavares, T. M., and Kesselmeier, J.: Exchange of  
1154 Short-Chain Aldehydes Between Amazonian Vegetation and the Atmosphere, *Ecol. Appl.*, 14, 247–262,  
1155 <https://doi.org/10.1890/01-6027>, 2004.
- 1156 Rottenberger, S., Kleiss, B., Kuhn, U., Wolf, A., Piedade, M. T. F., Junk, W., and Kesselmeier, J.: The effect of  
1157 flooding on the exchange of the volatile C<sub>2</sub>-compounds ethanol, acetaldehyde and acetic acid between leaves of  
1158 Amazonian floodplain tree species and the atmosphere, *Biogeosciences*, 5, 1085–1100, [https://doi.org/10.5194/bg-5-](https://doi.org/10.5194/bg-5-1085-2008)  
1159 1085-2008, 2008.
- 1160 Rummel, U., Ammann, C., Gut, A., Meixner, F. X., and Andreae, M. O.: Eddy covariance measurements of nitric  
1161 oxide flux within an Amazonian rain forest, *J. Geophys. Res. Atmospheres*, 107, LBA 17-1-LBA 17-9,  
1162 <https://doi.org/10.1029/2001JD000520>, 2002.
- 1163 Scala, A., Allmann, S., Mirabella, R., Haring, M. A., and Schuurink, R. C.: Green Leaf Volatiles: A Plant's  
1164 Multifunctional Weapon against Herbivores and Pathogens, *Int. J. Mol. Sci.*, 14, 17781–17811,  
1165 <https://doi.org/10.3390/ijms140917781>, 2013.
- 1166 Schade, G. W. and Goldstein, A. H.: Fluxes of oxygenated volatile organic compounds from a ponderosa pine  
1167 plantation, *J. Geophys. Res. Atmospheres*, 106, 3111–3123, <https://doi.org/10.1029/2000JD900592>, 2001.
- 1168 Sebbar, N., Bozzelli, J. W., and Bockhorn, H.: Thermochemistry and Reaction Paths in the Oxidation Reaction of  
1169 Benzoyl Radical: C<sub>6</sub>H<sub>5</sub>C(=O), *J. Phys. Chem. A*, 115, 11897–11914, <https://doi.org/10.1021/jp2078067>, 2011.





- 1170 Seco, R., Peñuelas, J., and Filella, I.: Short-chain oxygenated VOCs: Emission and uptake by plants and atmospheric  
1171 sources, sinks, and concentrations, *Atmos. Environ.*, 41, 2477–2499, <https://doi.org/10.1016/j.atmosenv.2006.11.029>,  
1172 2007.
- 1173 Singh, H. B., Herlth, D., O'Hara, D., Salas, L., Torres, A. L., Gregory, G. L., Sachse, G. W., and Kasting, J. F.:  
1174 Atmospheric peroxyacetyl nitrate measurements over the Brazilian Amazon Basin during the wet season:  
1175 Relationships with nitrogen oxides and ozone, *J. Geophys. Res. Atmospheres*, 95, 16945–16954,  
1176 <https://doi.org/10.1029/JD095iD10p16945>, 1990.
- 1177 Singh, H. B., Salas, L. J., Chatfield, R. B., Czech, E., Fried, A., Walega, J., Evans, M. J., Field, B. D., Jacob, D. J.,  
1178 Blake, D., Heikes, B., Talbot, R., Sachse, G., Crawford, J. H., Avery, M. A., Sandholm, S., and Fuelberg, H.: Analysis  
1179 of the atmospheric distribution, sources, and sinks of oxygenated volatile organic chemicals based on measurements  
1180 over the Pacific during TRACE-P, *J. Geophys. Res. Atmospheres*, 109, <https://doi.org/10.1029/2003JD003883>, 2004.
- 1181 Smith, D., Wang, T., and Španěl, P.: Analysis of ketones by selected ion flow tube mass spectrometry, *Rapid Commun.*  
1182 *Mass Spectrom.*, 17, 2655–2660, <https://doi.org/10.1002/rcm.1244>, 2003.
- 1183 Smith, D., Chippendale, T. W. E., and Španěl, P.: Selected ion flow tube, SIFT, studies of the reactions of H<sub>3</sub>O<sup>+</sup>,  
1184 NO<sup>+</sup> and O<sub>2</sub><sup>+</sup> with some biologically active isobaric compounds in preparation for SIFT-MS analyses, *Int. J. Mass*  
1185 *Spectrom.*, 303, 81–89, <https://doi.org/10.1016/j.ijms.2011.01.005>, 2011.
- 1186 Španěl, P. and Smith, D.: SIFT studies of the reactions of H<sub>3</sub>O<sup>+</sup>, NO<sup>+</sup> and O<sub>2</sub><sup>+</sup> with a series of volatile carboxylic  
1187 acids and esters, *Int. J. Mass Spectrom. Ion Process.*, 172, 137–147, [https://doi.org/10.1016/S0168-1176\(97\)00246-2](https://doi.org/10.1016/S0168-1176(97)00246-2),  
1188 1998.
- 1189 Španěl, P. and Smith, D.: SIFT studies of the reactions of H<sub>3</sub>O<sup>+</sup>, NO<sup>+</sup> and O<sub>2</sub><sup>+</sup> with several ethers, *Int. J. Mass*  
1190 *Spectrom. Ion Process.*, 172, 239–247, [https://doi.org/10.1016/S0168-1176\(97\)00277-2](https://doi.org/10.1016/S0168-1176(97)00277-2), 1998.
- 1191 Španěl, P., Ji, Y., and Smith, D.: SIFT studies of the reactions of H<sub>3</sub>O<sup>+</sup>, NO<sup>+</sup> and O<sub>2</sub><sup>+</sup> with a series of aldehydes and  
1192 ketones, *Int. J. Mass Spectrom. Ion Process.*, 165–166, 25–37, [https://doi.org/10.1016/S0168-1176\(97\)00166-3](https://doi.org/10.1016/S0168-1176(97)00166-3), 1997.
- 1193 Španěl, P., Wang, T., and Smith, D.: A selected ion flow tube, SIFT, study of the reactions of H<sub>3</sub>O<sup>+</sup>, NO<sup>+</sup> and O<sub>2</sub><sup>+</sup>  
1194 ions with a series of diols, *Int. J. Mass Spectrom.*, 218, 227–236, [https://doi.org/10.1016/S1387-3806\(02\)00724-8](https://doi.org/10.1016/S1387-3806(02)00724-8),  
1195 2002.
- 1196 Tani, A. and Hewitt, C. N.: Uptake of Aldehydes and Ketones at Typical Indoor Concentrations by Houseplants,  
1197 *Environ. Sci. Technol.*, 43, 8338–8343, <https://doi.org/10.1021/es9020316>, 2009.
- 1198 Tani, A., Tobe, S., and Shimizu, S.: Uptake of Methacrolein and Methyl Vinyl Ketone by Tree Saplings and  
1199 Implications for Forest Atmosphere, *Environ. Sci. Technol.*, 44, 7096–7101, <https://doi.org/10.1021/es1017569>, 2010.
- 1200 Trebs, I., Mayol-Bracero, O. L., Pauliquevis, T., Kuhn, U., Sander, R., Ganzeveld, L., Meixner, F. X., Kesselmeier,  
1201 J., Artaxo, P., and Andreae, M. O.: Impact of the Manaus urban plume on trace gas mixing ratios near the surface in  
1202 the Amazon Basin: Implications for the NO-NO<sub>2</sub>-O<sub>3</sub> photostationary state and peroxy radical levels, *J. Geophys. Res.*  
1203 *Atmospheres*, 117, <https://doi.org/10.1029/2011JD016386>, 2012.
- 1204 Villanueva, F., Tapia, A., Notario, A., Albaladejo, J., and Martínez, E.: Ambient levels and temporal trends of VOCs,  
1205 including carbonyl compounds, and ozone at Cabañeros National Park border, Spain, *Atmos. Environ.*, 85, 256–265,  
1206 <https://doi.org/10.1016/j.atmosenv.2013.12.015>, 2014.
- 1207 Villanueva-Fierro, I., Popp, C. J., and Martin, R. S.: Biogenic emissions and ambient concentrations of hydrocarbons,  
1208 carbonyl compounds and organic acids from ponderosa pine and cottonwood trees at rural and forested sites in Central  
1209 New Mexico, *Atmos. Environ.*, 38, 249–260, <https://doi.org/10.1016/j.atmosenv.2003.09.051>, 2004.





- 1210 Wang, C., Yuan, B., Wu, C., Wang, S., Qi, J., Wang, B., Wang, Z., Hu, W., Chen, W., Ye, C., Wang, W., Sun, Y.,  
1211 Wang, C., Huang, S., Song, W., Wang, X., Yang, S., Zhang, S., Xu, W., Ma, N., Zhang, Z., Jiang, B., Su, H., Cheng,  
1212 Y., Wang, X., and Shao, M.: Measurements of higher alkanes using NO<sub>2</sub><sup>+</sup> chemical ionization  
1213 in PTR-ToF-MS: important contributions of higher alkanes to secondary organic aerosols in China, *Atmospheric*  
1214 *Chem. Phys.*, 20, 14123–14138, <https://doi.org/10.5194/acp-20-14123-2020>, 2020a.
- 1215 Wang, M., Zhang, L., Boo, K. H., Park, E., Drakakaki, G., and Zakharov, F.: PDC1, a pyruvate/ $\alpha$ -ketoacid  
1216 decarboxylase, is involved in acetaldehyde, propanal and pentanal biosynthesis in melon (*Cucumis melo* L.) fruit,  
1217 *Plant J.*, 98, 112–125, <https://doi.org/10.1111/tpj.14204>, 2019.
- 1218 Wang, N., Edtbauer, A., Stöner, C., Pozzer, A., Bourtsoukidis, E., Ernle, L., Dienhart, D., Hottmann, B., Fischer, H.,  
1219 Schuladen, J., Crowley, J. N., Paris, J.-D., Lelieveld, J., and Williams, J.: Measurements of carbonyl compounds  
1220 around the Arabian Peninsula indicate large missing sources of acetaldehyde, *Gases/Field*  
1221 *Measurements/Troposphere/Chemistry* (chemical composition and reactions), <https://doi.org/10.5194/acp-2020-135>,  
1222 2020b.
- 1223 Warneck, P.; Williams, J.: *The Atmospheric Chemists Companion*, 1., Springer Verlag GmbH, 2012.
- 1224 Warneke, C., Karl, T., Judmaier, H., Hansel, A., Jordan, A., Lindinger, W., and Crutzen, P. J.: Acetone, methanol,  
1225 and other partially oxidized volatile organic emissions from dead plant matter by abiological processes: Significance  
1226 for atmospheric HO<sub>x</sub> chemistry, *Glob. Biogeochem. Cycles*, 13, 9–17, <https://doi.org/10.1029/98GB02428>, 1999.
- 1227 Williams, J., Fischer, H., Harris, G. W., Crutzen, P. J., Hoor, P., Hansel, A., Holzinger, R., Warneke, C., Lindinger,  
1228 W., Scheeren, B., and Lelieveld, J.: Variability-lifetime relationship for organic trace gases: A novel aid to compound  
1229 identification and estimation of HO concentrations, *J. Geophys. Res. Atmospheres*, 105, 20473–20486,  
1230 <https://doi.org/10.1029/2000JD900203>, 2000.
- 1231 Williams, J., Pöschl, U., Crutzen, P. J., Hansel, A., Holzinger, R., Warneke, C., Lindinger, W., and Lelieveld, J.: An  
1232 *Atmospheric Chemistry Interpretation of Mass Scans Obtained from a Proton Transfer Mass Spectrometer Flown over*  
1233 *the Tropical Rainforest of Surinam*, 2001.
- 1234 Wolfe, G. M., Thornton, J. A., McKay, M., and Goldstein, A. H.: Forest-atmosphere exchange of ozone: sensitivity  
1235 to very reactive biogenic VOC emissions and implications for in-canopy photochemistry, *Atmospheric Chem. Phys.*,  
1236 11, 7875–7891, <https://doi.org/10.5194/acp-11-7875-2011>, 2011.
- 1237 Xing, J.-H., Ono, M., Kuroda, A., Obi, K., Sato, K., and Imamura, T.: Kinetic Study of the Daytime Atmospheric Fate  
1238 of (Z)-3-Hexenal, *J. Phys. Chem. A*, 116, 8523–8529, <https://doi.org/10.1021/jp303202h>, 2012.
- 1239 Yamauchi, Y., Kunishima, M., Mizutani, M., and Sugimoto, Y.: Reactive short-chain leaf volatiles act as powerful  
1240 inducers of abiotic stress-related gene expression, *Sci. Rep.*, 5, 8030, <https://doi.org/10.1038/srep08030>, 2015.
- 1241 Yáñez-Serrano, A. M., Nölscher, A. C., Williams, J., Wolff, S., Alves, E., Martins, G. A., Bourtsoukidis, E., Brito, J.,  
1242 Jardine, K., Artaxo, P., and Kesselmeier, J.: Diel and seasonal changes of biogenic volatile organic compounds within  
1243 and above an Amazonian rainforest, *Atmospheric Chem. Phys.*, 15, 3359–3378, [https://doi.org/10.5194/acp-15-3359-](https://doi.org/10.5194/acp-15-3359-2015)  
1244 2015, 2015.
- 1245 Yáñez-Serrano, A. M., Nölscher, A. C., Bourtsoukidis, E., Derstroff, B., Zannoni, N., Gros, V., Lanza, M., Brito, J.,  
1246 Noe, S. M., House, E., Hewitt, C. N., Langford, B., Nemitz, E., Behrendt, T., Williams, J., Artaxo, P., Andreae, M.  
1247 O., and Kesselmeier, J.: Atmospheric mixing ratios of methyl ethyl ketone (2-butanone) in tropical, boreal, temperate  
1248 and marine environments, *Atmospheric Chem. Phys.*, 16, 10965–10984, <https://doi.org/10.5194/acp-16-10965-2016>,  
1249 2016.
- 1250 Yee, L. D., Isaacman-VanWertz, G., Wernis, R. A., Meng, M., Rivera, V., Kreisberg, N. M., Hering, S. V., Bering,  
1251 M. S., Glasius, M., Upshur, M. A., Gray Bé, A., Thomson, R. J., Geiger, F. M., Offenberg, J. H., Lewandowski, M.,  
1252 Kourtchev, I., Kalberer, M., de Sá, S., Martin, S. T., Alexander, M. L., Palm, B. B., Hu, W., Campuzano-Jost, P., Day,



- 1253 D. A., Jimenez, J. L., Liu, Y., McKinney, K. A., Artaxo, P., Viegas, J., Manzi, A., Oliveira, M. B., de Souza, R.,  
1254 Machado, L. A. T., Longo, K., and Goldstein, A. H.: Observations of sesquiterpenes and their oxidation products in  
1255 central Amazonia during the wet and dry seasons, *Atmospheric Chem. Phys.*, 18, 10433–10457,  
1256 <https://doi.org/10.5194/acp-18-10433-2018>, 2018.
- 1257 Yee, L. D., Goldstein, A. H., and Kreisberg, N. M.: Investigating Secondary Aerosol Processes in the Amazon through  
1258 Molecular-level Characterization of Semi-Volatile Organics, Univ. of California, Berkeley, CA (United States),  
1259 <https://doi.org/10.2172/1673764>, 2020.
- 1260 Zannoni, N., Wikelski, M., Gagliardo, A., Raza, A., Kramer, S., Seghetti, C., Wang, N., Edtbauer, A., and Williams,  
1261 J.: Identifying volatile organic compounds used for olfactory navigation by homing pigeons, *Sci. Rep.*, 10, 15879,  
1262 <https://doi.org/10.1038/s41598-020-72525-2>, 2020a.
- 1263 Zannoni, N., Leppla, D., Lembo Silveira de Assis, P. I., Hoffmann, T., Sá, M., Araújo, A., and Williams, J.: Surprising  
1264 chiral composition changes over the Amazon rainforest with height, time and season, *Commun. Earth Environ.*, 1, 1–  
1265 11, <https://doi.org/10.1038/s43247-020-0007-9>, 2020b.